N° Ordre........../FT/UMBB/2024

PEOPLE'S DEMOCTRATIC REPUBLIC OF ALGERIA
MINISTRY OF HIGHER EDUCATION AND SCIENTIFIC RESEARCH
M'HAMED BOUGARA UNIVERSITY OF BOUMERDES

Faculté of Technology

Doctorate Thesis

Presented by:

MAHAMI Amine

Submitted for the fulfillment of the requirements of the **Doctorate - LMD degree** in

Field: Electromechanics

Speciality: Mechatronics

Electrical systems faults diagnosis based on thermography and machine learning techniques

Before the jury composed of:

M. ADJERID	Smaïl	Professor	UMBB	Chairman
M. BENAZZOUZ	Djamel	Professor	UMBB	Thesis Director
M. RAHMOUNE	Chemesddine	Professor	UMBB	Thesis Co-director
M. BENTARZI	Hamid	Professor	UMBB	Examiner
M. BENFDILA	Arezki	Professor	UMMTO	Examiner
M. GOURI	Rabeh	Professor	ENSTA	Examiner

Année Universitaire 2023/2024

Acknowledgement

I owe ALLAH (God) a debt of gratitude and thanks for giving me the forbearance, blessings, and endurance that allowed me to complete this work in spite of the difficult conditions in my native Algeria.

This thesis represents the result of almost four years of study that I did at the Faculty of Technology (FT) Solid Mechanics and Systems Laboratory for my doctoral studies. I am appreciative of Professor Benazzouz Djamel for giving me the chance to work toward my PhD in this fascinating area of study, as well as for his thoughtful advice and supportive attitude. I sincerely thank Associate Professor Rahmoune Chemesddine, my supervisor, for his wise counsel, perceptive criticism, and unfailing support. Together, we have had in-depth and insightful conversations about how to best present my research. I am appreciative of our time together because it has helped me comprehend electromechanical machinery better.

I also want to thank my buddies at LMSS and all of my coworkers in our division for their support and the priceless memories we have made together. I would especially like to thank my friends for supporting me during my doctoral journey.

MAHAMI Amine

February; 2024

Electrical systems faults diagnosis based on thermography and machine learning techniques.

Abstract

The goal of using AI-driven conditional monitoring in electrical devices is to monitor and trace the beginning and development of deterioration prior to a failure. This degradation eventually results in a system malfunction that impacts the availability of the whole system. Early identification allows for a planned shutdown, averting catastrophic failure and guaranteeing more cost-effective and dependable operation.

This study is divided into two major parts: the first part deals with the identification and categorization of faults in induction motors, and the second part deals with the detection and classification of faults in transformers.

In machine health management, condition monitoring and problem diagnostics of electrical machines are important study areas. Using infrared thermography method (IRT), a new noncontact and nonintrusive experimental framework is used in the first portion of this thesis to monitor and diagnose defects in a three-phase induction motor. Using IRT to obtain a thermograph of the target machine is the first step in the process. The Speeded-Up Robust Features (SURF) detector and descriptor are then used to extract fault features from the IRT images using the bag-of-visual-word (BoVW) technique. Then, a group learning method known as Extremely Randomized Tree (ERT) is applied to automatically detect different types of induction motor defect patterns. Based on experimental IRT images, the efficacy of the suggested method is evaluated, showcasing its potential as a potent diagnostic tool with superior classification accuracy and stability over alternative approaches.

The second part of the thesis presents an experimental framework that uses infrared thermography (IRT) to monitor and diagnose transformer defects in a non-intrusive and non-contact manner. Using IRT to obtain a thermograph of the intended machine is the first step in the process. GIST features are then taken from the database's reference image and every other image. Finally, a machine learning technique known as Support Vector Machine (SVM) is used to automatically identify different fault patterns in the transformer. Based on experimental IRT images and diagnostic results, the efficacy and capacity of the proposed method are assessed, demonstrating its potential as a potent diagnostic tool with high classification accuracy and stability. This method improves operational reliability by facilitating the early identification and detection of transformer failures.

Keywords

Infrared thermography images, induction motor, electrical transformer, faults diagnosis, feature extraction, extremely randomized tree, support vector machine, faults classification stability, machine learning.

Diagnostic des défauts des systèmes électriques basé sur des techniques de thermographie et d'apprentissage automatique.

Résumé

L'objectif de la surveillance conditionnelle basée sur l'intelligence artificielle dans les machines électriques est de surveiller l'apparition et l'évolution d'une dégradation avant qu'une panne ne survienne. La dégradation entraînera à terme un dysfonctionnement du système (moteur à induction ou transformateur), ce qui se répercutera sur la disponibilité de l'ensemble du système. Une détection précoce permet un arrêt planifié approprié pour éviter une panne catastrophique et, par conséquent, un fonctionnement plus fiable et un coût moindre.

Ce travail de recherche s'articule sur deux parties essentielles : la première partie concerne la détection et la classification des défauts dans les moteurs asynchrones, et la seconde partie se concentre sur la détection et la classification des défauts dans les transformateurs.

La surveillance conditionnelle et le diagnostic des défauts des machines électriques sont des thèmes de recherche très importants dans le domaine de la gestion de l'état des

machines. Dans cette thèse, dans un premier temps, une nouvelle méthode expérimentale sans contact et non intrusive est utilisée pour la surveillance et le diagnostic des défauts d'un moteur à induction triphasé basée sur une technique de thermographie infrarouge (IRT). La structure de base de ce travail commence par l'application de l'IRT pour obtenir un thermographe de la machine considérée. Ensuite, le bag-of-visual-word (BoVW) est utilisé pour extraire les caractéristiques de défaut avec le détecteur et le descripteur Speeded-Up Robust Features (SURF) des images IRT. Enfin, divers modèles de défauts dans le moteur à induction sont automatiquement identifiés à l'aide d'un apprentissage d'ensemble appelé arbre extrêmement aléatoire (ERT). L'efficacité de la méthode proposée est évaluée sur la base des images IRT expérimentales, et les résultats du diagnostic montrent sa capacité et qu'elle peut être considérée comme un outil de diagnostic puissant avec une précision et une stabilité de classification élevées par rapport aux autres méthodes précédemment utilisées.

De plus, la deuxième partie de cette thèse traite aussi une nouvelle méthode expérimentale sans contact et non intrusive utilisée pour la surveillance et le diagnostic des défauts des transformateurs basée sur une technique de thermographie infrarouge (IRT). La structure de base de ce travail commence par l'application (IRT) pour obtenir un thermographe de la machine considérée. Deuxièmement, les caractéristiques GIST de l'image de référence et de toutes les images de la base de données d'images sont extraites. Enfin, divers modèles de défauts dans le transformateur sont automatiquement identifiés à l'aide d'une méthode d'apprentissage automatique appelée Support Vector Machine (SVM).

L'efficacité et la capacité de la méthode proposée sont évaluées sur la base des images expérimentales de thermographie infrarouge (IRT) et des résultats du diagnostic en identifiant neuf types d'états de transformateur électrique parmi lesquels un est sain et les huit autres sont des défauts de court-circuit dans le type d'enroulement du noyau commun, et montrant qu'il peut être considéré comme un outil de diagnostic puissant avec une précision et une stabilité de classification élevées, et qu'il permet de détecter et d'identifier les défauts à un stade précoce.

Mots-clés

Images de thermographie infrarouge, moteur à induction, transformateur électrique, diagnostic de défauts, extraction de caractéristiques, arbre extrêmement aléatoire, machine à vecteurs de support. stabilité de la classification des défauts, apprentissage automatique.

تشخيص أعطال الأنظمة الكهربائية استنادًا إلى تقنيات التصوير الحراري والتعلم الآلي.

الملخص.

الهدف من المراقبة المشروطة المعتمدة على الذكاء الاصطناعي في الآلات الكهربائية هو مراقبة بداية التدهور وتطوره قبل حدوث الفشل. سيؤدي التدهور في النهاية إلى خلل في النظام)المحرك التعريفي أو المحول(، مما سيؤثر على توفر النظام بأكمله. يسمح الاكتشاف في مرحلة مبكرة بإيقاف التشغيل المخطط له بشكل مناسب لتجنب الفشل الكارثي، ونتيجة لذلك، تشغيل أكثر موثوقية وتكلفة أقل.

ينقسم هذا البحث إلى قسمين أساسيين: الجزء الأول يتعلق بالكشف عن الأعطال في المحركات الحثية وتصنيفها، أما الجزء الثاني فيركز على كشف وتصنيف الأعطال في المحولات.

تعد مراقبة حالة الآلات الكهربائية وتشخيص أعطالها من المواضيع البحثية المهمة جدًا في مجال إدارة صحة الآلة. في هذه الأطروحة، في البداية، تم استخدام طريقة تجريبية جديدة غير تلامسية وغير تدخلية لرصد وتشخيص أعطال المحرك التعريفي ثلاثي الطور استنادًا إلى تقنية التصوير الحراري بالأشعة تحت الحمراء للحصول على رسم حراري للآلة قيد النظر. بعد ذلك، يتم IRT يبدأ الهيكل الأساسي لهذا العمل بتطبيق (IRT). لاستخراج ميزات الخطأ باستخدام كاشف وواصف الميزات اليوقة (WVoB) استخدام حقيبة الكلمات المرئية وأخيرً ا، يتم تحديد أنماط الأعطال المختلفة في المحرا كالتعريفي تلقائيًا TRI. من صور(FRUS) السعيرة تم تقييم فعالية الطريقة المقترحة بناء على (TRE). باسدختام التعلم المجمعي الذي يسمى الشجرة العشويئاة للغاية التجريبية، وأظهرت نتائج التشخيص قدرتها وأنه يمكن ابتعارها أداة تشخيصية قوية ذات دقة تصنيف TRI صور عالية وثبات مقارنة بالطرق الأخرى المستخدمة سابقا.

كذلك، يتناول الجزء الثاني من هذه الأطروحة طريقة تجريبية جديدة غير تلامسية وغير تدخلية تستخدم لمراقبة يبدأ الهيكل .(IRT) وتشخيص أعطال المحولات بناءً على تقنية التصوير الحراري بالأشعة تحت الحمراء للحصول على مخطط حراري للآلة قيد النظر. ثانيًا، يتم استخراج ميزات (IRT) الأساسي لهذا العمل بتطبيق للصورة المرجعية وجميع الصور الموجودة في قاعدة بيانات الصور. أخيرًا، يتم تحديد أنماط الأعطال GIST

يتم تقييم فعالية وقدرة .(SVM) المختلفة في المحول تلقائيًا باستخدام طريقة التعلم الآلي التي تسمى آلة ناقل الدعم ونتائج التشخيص (IRT) الطريقة المقترحة بناءً على الصور التجريبية للتصوير الحراري بالأشعة تحت الحمراء من خلال تحديد تسعة أنواع من حالات المحولات الكهربائية، من بينها واحدة سليمة والثمانية المتبقية هي من أخطاء الدائرة القصيرة في نوع اللف الأساسي المشترك، وإظهار أنه يمكن اعتباره أداة تشخيصية قوية تتمتع بدقة تصنيف وثبات عالية، وتجعل من الممكن اكتشاف الأخطاء وتحديدها في مرحلة مبكرة.

الكلمات المفتاحية

الصور الحرارية بالأشعة تحت الحمراء، المحرك التعريفي، المحولات الكهربائية، تشخيص الأعطال، استخلاص الخصائص، الشجرة العشوائية للغاية، آلة ناقل الدعم. استقرار تصنيف الأخطاء، والتعلم الآلي.

Table of contents

List of Figures

List of Tables

Chapter 1: introduction

1.1 Background

Electromechanical systems are integral components in a wide range of industries, including automotive, aerospace, manufacturing, and robotics. These systems combine electrical and mechanical processes to perform complex tasks, making them essential for modern technological advancements. However, the complexity of EMS makes them susceptible to various faults and failures, which can lead to significant operational downtime, increased maintenance costs, and even safety hazards.

In general, there are many types of electrical machines in different power range and duty cycle classes. Notably, three-phase induction motors and electrical transformers that stand out as crucial and often used components among necessities. These machines are operated in industrial or civil operations, among which induction motors are considered as a powerful and mandatory driving machines in many commercial and industrial applications: Lifts, cranes, hoists, big exhaust fans, lathes, crushers, mills for oil extraction, and city eco-friendly electric and hybrid cars. Furthermore, electrical transformers have their part of necessity in power transportation and exploitation, they play a crucial role in electrical systems which makes them the main equipment for electrical transmission and distribution. Considering the importance of such equipment, one must take into account its eventual break down and its negative impact not only on the machine itself, but on the whole production chain and the productivity of the factory. Therfore, It is necessary to evaluate the failure rates and their distribution on certain types of electrical machines and their subsystems.

From the analysis based on publicly available data, summaries and compares the results obtained from studies carried out in recent years. It can be stipulated that [1] most encountered problems in induction motors exists in stator winding (60%). On the other hand, core windings are considered the most defective components in electrical transformers with a rate of 34%.

Traditional methods for diagnosing faults in electromechanical systems often rely on manual inspections and predetermined maintenance schedules. Recently, vibration signal analysis has been the most widely used method to monitor induction motors and diagnose their faults. Several signal processing techniques have been developed such as those published by Zair et al. [2]; Bettahar et al. [3]; Nayana et al.[4]; Glowacz et al.[5].

Since vibration is considered a non-avoidable phenomenon in dynamic systems, the isolation and the diagnosis of combined faults is generally difficult and not easy to establish due to the complexity of the structure and the machinery multiple components interactions. For this purpose, accelerometers are usually needed. However, they require being in contact with the object that needs to be monitored. Multiple challenges are encountered and must be considered before the installation of accelerometers, namely the high operating temperatures and greasy surfaces.

In addition, the external short circuit is one of the most common failures of electrical transformers [6]. This led the scholars to develop more reliable monitoring techniques and fast diagnosis tools with low cost. For that reason, scholars solved many issue related to transformer winding short circuit faults, by developing various techniques such as low voltage impulse method (LVI)[7-8], short-circuit reactance measurement (SCR) [9], frequency response analysis technique (FRA)[10], sweep frequency impedance method (SFI)[11], and Dissolved Gas Analysis (DGA)[12]; but unfortunately, those techniques has majors disadvantage such as: their fact of being offline methods and require power cuts, DGA need oil sampling and analyzing which are not flexibles.

In the last decade, researchers developed methods by using non-invasive analysis techniques such as the acoustic methods for winding short-circuit fault diagnosis [13], which can be applied while the equipment is in operation. This approach has been widely used to monitor the electrical transformer and fault diagnosis. However, its use is not appropriate in this case for the effect of acoustic emission environment, or other nearby electrical devices equipment, mainly caused by the magneto-astrictive action of the core, Barkhausen noise, oil pumps, and cooling fans. Generally, these techniques, which use the effect of acoustic propagation signal, complicates the task of transformer fault detection, and can be considered as major limitation of acoustic analysis in fault transformer diagnosis.

Most of the methods presented before are not flexible for the diagnostic of electromechanical systems, especially induction motors and electrical transformer. This led us to look for an efficient and fast method to monitor and diagnose these machines. Consequently, there is a growing need for more sophisticated , non-invasive and reliable diagnostic techniques that can enhance the efficiency and reliability of these systems.

For that reason, in this thesis, a new intelligent thechnique, based infrared thermal imaging, which is a non-contact, non-intrusive measurement technique that can detect all temperature variations of the monitored system components and the Artificial Intelligence (AI) tools, is proposed to diagnose faults in electromechanical systems.

1.2 Research motivation

The appearance of a fault in any electromechanical systems such as induction motors and electrical transformers can lead to replacement costs, production downtime and even loss of human life, so it is essential to avoid these failures. For this reason, it is necessary to identify and develop a prevention techniques or systems that can detect of a defect before their total failure .

A. Case study : induction motors

The diagnosis of induction motors is considered one of the most important disciplines in electromechanical systems. In recent years, many methods have been developed to detect and diagnose faults in this equipment. This presents a new challenge to develop methods to keep motors in good technical condition under various operating modes (different fault sizes).

- Detecting and classifying induction motor faults for different severity grades of short circuits in the stator windings (0%, 10%, 30%, 50%) is difficult, especially when the differentiation between faults severity and grades becomes hard and misleading.
- Detecting and locating faults in asynchronous motors for each faulty phase of the machine and sometimes several phases (A, A&B, A&B&C) is also difficult and requires more attention and accurate tools to detect and diagnose.

- Therefore, the use of the infrared thermography technique alone does not meet the needs; which brought us back to propose in this research work a new technique that uses infrared thermography combined with artificial intelligence; A suitable method for detecting and differentiating among various states of faults in induction motors.

B. Case study: electrical transformers

The most critical failure of an electrical transformer is common core winding failures. This has led researchers to develop more reliable monitoring technique, rapid and inexpensive diagnostic tools. To overcome these issues, infrared thermography is a non-contact, non-intrusive measurement technique capable of detecting all temperature variations of the monitored system components. This technique has been widely used in non-destructive examination and it is known that valuable information is contained in IRT images and can be used as a diagnostic tool to resolve the problem, but:

- Detecting and classifying electrical transformer faults in common core winding for different severity cases of short circuits rounds (0%,13% … 100%) is difficult especially the differentiation among fault cases and can be misleading.
- Detecting and locating the transformer fault in the common core winding and not affecting other components, is also difficult to differentiate and can be lead misleading results.

In this research work, a new effective and reliable approach based on infrared thermography and artificial intelligence is proposed, to solve the problems and detect various states of faults in the common core winding of machine.

1.3 Research objective

There are many works in the literature dealing with the search for better fault detection methods in electromechanical machines, especially induction motors and electrical transformers, which are essential equipment that play an important role in industries. It is therefore necessary to find an effective and reliable method to detect its failure.

- **At first**

Many methods have been developed to improve the identification of faults in induction motors, among which machine learning (ML) has become a prominent tool for this purpose. Furthermore, the diagnostic procedure incorporates Infrared thermal imaging, a noncontact and nonintrusive monitoring technology that may identify temperature fluctuations in all monitored system components. This thesis uses Infrared Thermal Imaging (IRT) to obtain a thermograph of the targeted area in order to begin investigating this issue.

This work aims to present a novel intelligent method for the diagnosis of induction motor faults using Infrared Thermal Imaging (IRT), Extremely Randomized Tree (ERT) classifier, and image feature extraction using the Bag-of-Visual-Word (BoVW) and Speeded-Up Robust Features (SURF) techniques.

- **In the second**

The goal of this research is to lessen significant damage, stop unintentional power outages, and lessen the need for expensive remedial repair. This is accomplished by focusing emphasis on the monitoring of electrical transformers, which are essential parts of electrical systems and the main apparatus used for distribution and transmission. Using infrared thermography technique (IRT) in the study presents a novel noncontact and non-intrusive experimental framework for monitoring and diagnosing transformer failures.

The first step is to use infrared thermography (IRT) to take thermographs of the transformer that is the target. After that, all other photos in the database as well as the reference image have their GIST features extracted. Then, a machine learning method called Support Vector Machine (SVM) is used to automatically detect different types of transformer fault patterns. Experimental IRT images are used to evaluate the efficacy and capabilities of the proposed method, which shows that it is capable of distinguishing nine different states of electrical transformers. Of these, one represents a healthy state while the other eight represent common short-circuit problems of the core winding type. The suggested method's outstanding classification accuracy and stability are demonstrated by a comparative study with previously employed approaches, demonstrating its effectiveness as a trustworthy diagnostic tool.

The objectives of this study are:

- A. To propose a new method for diagnosing faults in both three-phase induction motors and electrical transformers by combining the use of infrared thermal imaging with machine learning to automate the classification of faults.
- B. A novel effective feature extraction method for three-phase induction motors and electrical transformers faults diagnosis based on thermal imaging.
- C. Use a powerful classifier to improve fault classification for different fault sizes, as well as increase the accuracy and stability of the diagnostic system.

1.4 Thesis organization

The five chapters that make up this thesis are as follows:

This thesis begin with a general introduction, then an overview of electromechanical systems is given in Chapter 2, with a particular emphasis on electrical transformers and induction motors. The chapter begins by highlighting the vital nature of their applications, then it examines the several types of problems that can interfere with their regular operations and the technologies used to monitor them. A review of existing research on widely applied infrared thermography methods for transformer and induction motor diagnosis is also done. Three processes make up the diagnosis process: (1) gathering thermographic images from actual experiences; (2) extracting fault features; and (3) classifying states using artificial intelligence methods. Furthermore, a thorough explanation of the suggested approach created in this thesis is given.

The fundamentals of image processing are covered in Chapter 3, along with how to use it to extract features from infrared pictures of electrical transformers and induction motors that were taken during experiments.

An overview of artificial intelligence methods and their uses, mainly in the field of categorization, is provided in Chapter 4.

The experimentally acquired datasets for the machines under consideration, which include various fault modes, severity levels, and nominal conditions, are described in Chapter 5. Sturdy traits are retrieved, and a thorough analysis is done to compare the developed techniques with an industry standard. Automatic fault identification and classification is accomplished by selecting and utilizing machine learning classifiers.

The thesis is concluded in Chapter 6, where important contributions are summarized, the relevance of the results discussed, and future study directions are suggested.

Chapter 2: Infrared thermography and diagnosis

2.1 Introduction

The scientific field of infrared radiation thermography (IRT) is devoted to the acquisition and analysis of thermal data through the use of non-contact measurement instruments [14]. It is based on electromagnetic energy known as infrared, which is located below the red end of the spectrum and has longer wavelengths than visible light. Any object that is warmer than absolute zero ($T > 0$ K) will produce infrared radiation [15]. Since this kind of radiation is invisible to the human eye, data collection and analysis involving infrared measuring instruments is required [16].

2.2 History and infrared radiation origin

Mr William Herschel, a British astronomer, made a significant discovery about infrared radiation in 1800. He performed an experiment in which a thermometer slightly placed beyond the visible spectrum and let sunlight flow through a prism. The temperature that was measured was noticeably higher. When sunlight comes into contact with your skin, you'll feel something similar to what Herschel observed in his experiment. In this case, the energy that is interpreted as heat is released when infrared radiation causes the bonds between molecules to shift [17].

2.3 Infrared radiation physics

The infrared radiation that an item emits is detected by infrared measurement equipment, which then transform it into an electrical signal [14]. The pyrometer is a basic infrared device that uses a single sensor to produce a single output. More sophisticated gadgets use a variety of sensors to produce an intricate infrared picture of the environment. An infrared image shows the scene itself as the source and may be seen by an infrared camera without the need for light, in contrast to a visible image that shows reflected light on the scene. A thermogram, a false-color image, is produced by giving each infrared energy level a color in order to convert photos taken with infrared cameras into visible images [18].

A surface that is warmer than absolute zero releases energy known as infrared radiation [19]. The amount of radiation released is directly correlated with the temperature of the substance; greater temperatures cause the infrared energy released to be more intense.

Three ways exist for dissipating radiant energy that strikes an object: absorption, transmission, and reflection [14]. The absorptivity, transmissivity, and reflectivity of the body are the percentages of total radiant energy linked to each of these dissipation processes.

The spectral absorptance ($\alpha\lambda$) indicates the ratio of spectral radiant power absorbed by the object; the spectral reflectance ($\rho\lambda$) indicates the ratio of spectral radiant power reflected by the object; and the spectral transmittance ($\tau\lambda$) indicates the ratio of spectral radiant power transmitted by the object. These three parameters that characterize these phenomena. Since, wavelength affects all three parameters. Equation (1.1) states that at any given wavelength, their aggregate must equal to one.

$$\alpha_\lambda + \rho_\lambda + \tau_\lambda = 1 \qquad (2.1)$$

Equation (1) can be reduced to Equation (1.2) for opaque materials, indicating that all incident energy is absorbed or reflected. In other words, thae energy that is not absorbed is reflected.

$$\alpha_\lambda = 1 - \rho_\lambda \qquad (2.2)$$

Blackbodies are materials that have zero transmissivity and reflection. All incident radiant energy is absorbed ($\alpha\lambda = 1$) in these materials.

Equation (1.3) can be used to calculate the electromagnetic radiation emitted from a blackbody ($W\lambda b$). The result of Planck's law, which depends on both λ and T, is the power released per unit area per unit wavelength.

$$W_{\lambda_b} = \frac{c_1 \lambda^{-5}}{\lambda T \;\left(\frac{c_2}{}\right) - 1} \qquad (2.3)$$

where λ is the wavelength, T is the temperature, and C1 and C2 are constants

The dispersion of electromagnetic radiation that a blackbody emits at different temperatures is shown in Figure 1. The energy radiated at each wavelength is represented by the curves. It is clear that for a hotter object, the curve's peak has greater significance. Moreover, there is an inverse correlation between the emission peak's wavelength and temperature.

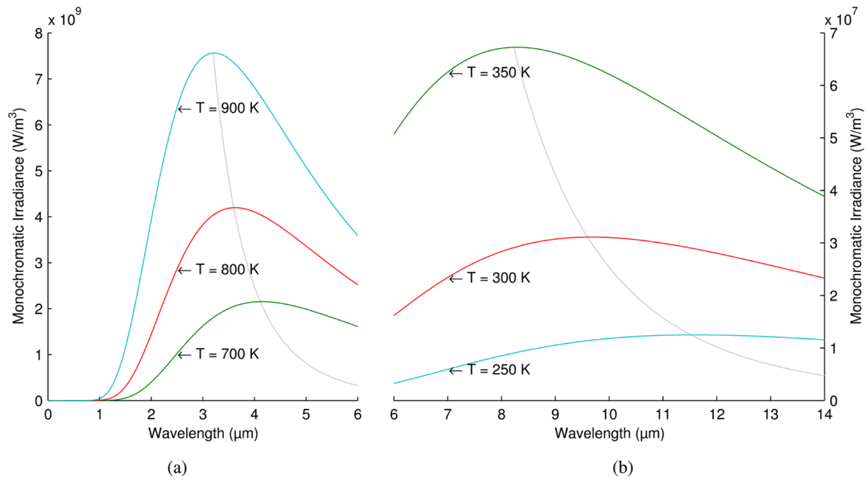

Figure 2.1. Planck's law electromagnetic radiation at different temperatures

Planck's law is shown in Figure 2.1, which also shows the electromagnetic radiation that a blackbody in thermal equilibrium at a given temperature would emit. (a) The bulk of radiation emitted by objects is in the mid-wave infrared; (b) the majority of radiation emitted by objects is in the long-wave infrared. It is significant to observe that the graph's two segments have distinct y-axis scales [17].

The temperature of the object determines the wavelength at which electromagnetic radiation is released; shorter wavelengths are produced at higher temperatures. There is displacement of the wavelength but the distribution stays the same. The peak wavelength for a given temperature value can be calculated using Wien's law, which is represented in Equation (2.4). The link between temperature and peak wavelength is shown graphically in Figure 2.1 using a logarithmic scale. By differentiating Planck's law in Equation (2.3) with respect to λ and determining the wavelength that corresponds to the maximum radiation intensity, Wien's law can be obtained [14].

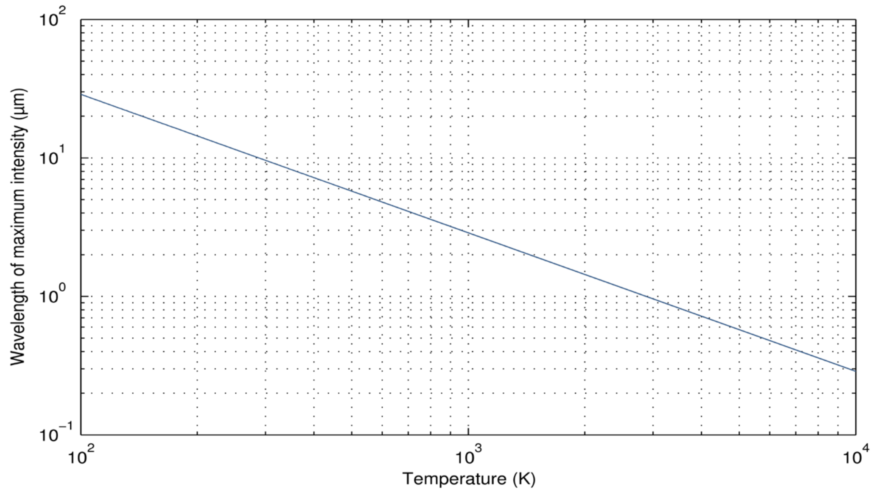

Figure 2.2. The wavelength maximum radiation intensity.

The wavelength at which a blackbody produces its maximum radiation intensity at a given temperature is determined by Wien's Displacement Law [14].

$$\lambda peak = 0.0029\, T \qquad (2.4)$$

Equation (2.5), where σ is a constant, is obtained by integrating Equation (2.3) over all wavelengths (λ) from zero to infinity in order to get the total hemispherical radiation intensity of a blackbody. The Stefan–Boltzmann formula is the name given to this expression.

$$W_b = \sigma\, T^4 \qquad (2.5)$$

Equation (3.6) defines the emissivity of a body at a wavelength λ as the ratio of the radiant energy released by the body to the radiation that a blackbody at the same temperature would emit.

$$\varepsilon_\lambda = \frac{W\lambda}{W\lambda b} \qquad (2.6)$$

At the same temperature, a real body emits only a fraction of the thermal energy that a blackbody emits. A body is called a greybody when its emissivity is constant and does not change with wavelength. Equation (3.7) can be used to define this condition:

$$\varepsilon_\lambda = \frac{W\lambda}{W\lambda b} = \frac{W}{Wb} = \varepsilon \qquad (2.7)$$

Real things can't be considered graybodies because their emissivity isn't constant or wavelength-independent. However, it is generally accepted that emissivity can be considered constant over short wavelength intervals. It is easier to treat real objects as graybodies when this assumption is made. Real objects are not considered true graybodies because their emissivity varies with wavelength; instead, their emissivity is averaged across brief intervals to match the operating range of infrared sensors. The gradual variation of emissivity as a function of wavelength for solid materials makes this averaging possible. This method might not work in other situations, such those involving gasses or liquids [20].

We get (2.8) by changing (2.7) into (2.5). The Stefan–Boltzmann formula for graybody radiators is represented by this equation. A graphic depiction of this formula for different emissivities is shown in Figure 2.3

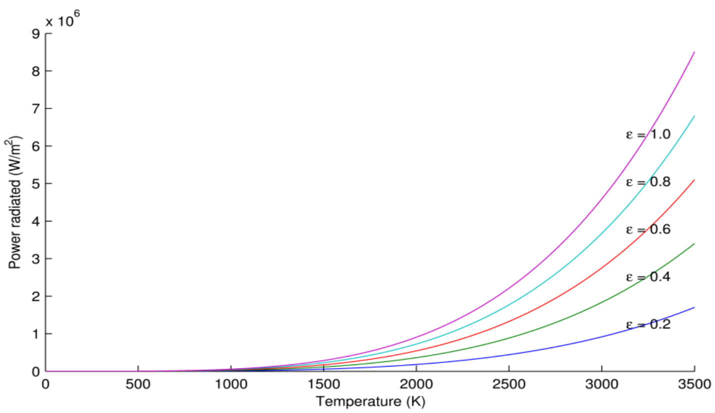

Figure 2.3 Power graybody with different emissivities according to Stefan-Boltzmann law [14].

$$W = \varepsilon \sigma T^4 \tag{2.8}$$

An item has a value of one absorptivity when 100% of the incident radiation energy is absorbed by it, with no transmission or reflection. Such a body has an emissivity of one since all absorbed energy must be reradiated (emitted) at a constant temperature. As a result, absorptivity and emissivity in a blackbody are equal and one. Kirchhoff's law states that a material's absorptivity and emissivity are always equal at a given temperature and wavelength. Equation (2.9) can be used to express this relationship:

$$\varepsilon_\lambda = \alpha_\lambda \tag{2.9}$$

Equation (2.10) for opaque materials can be found from Equations (2.9) and (2.2).

$$\rho_\lambda = 1 - \varepsilon_\lambda \qquad (2.10)$$

Only a small percentage of the thermal energy released by an analogous blackbody is released by graybodies. As a result, these bodies always have reflectivity more than zero and emissivity less than one [17].

2.4 Infrared radiation bands

The electromagnetic spectrum is divided into several regions or bands according to the wavelength. Regions are not sharply defined, and they differ in different disciplines. The infrared region is approximately defined from 0.8 μm to 1000 μm, that is, from the end of visible light to microwaves [14].

Much of the infrared range of the electromagnetic spectrum is not useful in IRT, because it is blocked by the atmosphere. The remaining portions define the usable part of the infrared by IRT [16]:

- Near-infrared (NIR) from 0.8 μm to 1.7 μm.
- Short-wavelength infrared (SWIR) from 1 μm to 2.5 μm.
- Mid-wavelength infrared (MWIR) from 2 μm to 5 μm.
- Long-wavelength infrared (LWIR) from 8 μm to 14 μm.

Among all of these regions, MWIR and LWIR are the most commonly used in IRT. There are two reasons: the band of peak emissions and atmospheric transmittance. The first reason is due to the relation between temperature and wavelength. The most effective measurement for a particular temperature should be carried out for the wavelength at which most intensity is emitted (see Figure 3.1). Measuring at a different wavelength would require a much more sensitive camera to achieve identical performance. Thus, for most applications, wavelengths longer than SWIR are required. The second reason is related to the atmospheric transmittance. Infrared radiation travels through air, being absorbed by various air particles, mostly by CO2 and H2O. The degree to which air absorbs infrared radiation depends on the wavelength. In the MWIR and LWIR bands, this absorption is low, allowing more radiation to reach the sensor of the camera.

Figure 4 shows the atmospheric transmittance for different wavelengths. As can be noticed, in the visible part of the spectrum, from 0.4 μm to 0.7 μm, only 60% of the emitted radiation is transmitted. However, between 5 μm and 7.5 μm, almost no radiation is transmitted. The atmosphere absorbs all of this radiation. Therefore, infrared measuring devices use either MWIR or LWIR. MWIR devices are used for high-temperature readings, while LWIR is used for ambient temperatures.

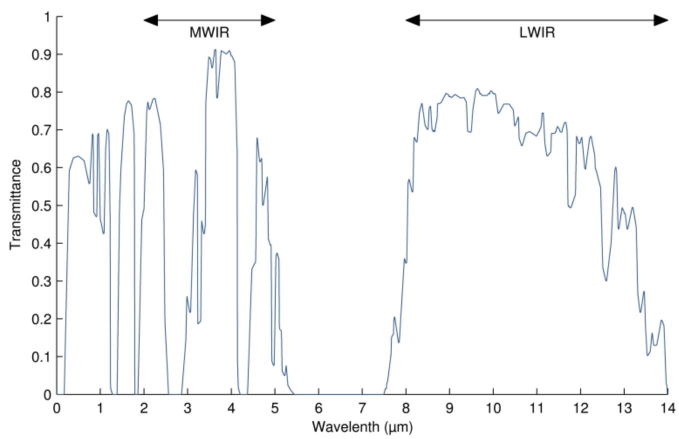

Figure 2.4 Atmospheric transmittance for different wavelengths [14].

2.5 Infrared thermography

Infrared thermography is a non-destructive testing technique that utilizes infrared radiation to detect, measure, and analyze temperature variations on the surface of objects or materials. This technique relies on the principle that all objects emit infrared radiation as a function of their temperature. By capturing and interpreting these thermal emissions, infrared thermography enables the visualization and quantification of temperature distributions, which can be indicative of various phenomena, including defects, anomalies, or operational conditions.

2.5.1 Basic Principles

The basic principle of infrared thermography is rooted in the laws of thermodynamics and the behavior of electromagnetic radiation. According to Planck's law of black-body radiation, all objects with a temperature above absolute zero emit electromagnetic radiation across a broad spectrum of wavelengths. The intensity and spectral distribution of this radiation depend on the object's temperature and emissivity.

Infrared thermography focuses on the infrared portion of the electromagnetic spectrum, typically spanning wavelengths from approximately 0.7 to 1000 micrometers. Within this range, objects emit thermal radiation predominantly in the long-wave infrared (LWIR) region, typically between 8 and 14 micrometers [20].

2.5.2 Operating Principle

Infrared cameras operate on the principle of detecting infrared radiation, which is emitted by objects due to their temperature. This radiation falls within the infrared portion of the electromagnetic spectrum, which is beyond the range of visible light [19].

Infrared thermography operates on the principle of measuring with an infrared camera the infrared radiation emitted by objects and converting it into temperature data. This process involves several key steps:

- Infrared Imaging: An infrared camera equipped with a detector sensitive to infrared radiation captures thermal images of the object or material under inspection. The camera detects the emitted radiation and converts it into electrical signals, which are then processed to generate a thermal image.
- Temperature Measurement: The thermal image depicts temperature variations across the surface of the object, with different colors or shades representing different temperature levels. The camera's sensitivity and calibration enable accurate temperature measurements within the observed scene.

- Analysis and Interpretation: Thermal images are analyzed and interpreted to identify patterns, anomalies, or areas of interest. By comparing temperature distributions and variations, anomalies such as hotspots, cold spots, or thermal gradients can be detected.

2.5.3 Infrared camera

The key component of an infrared camera is its infrared sensor. This sensor is typically a semiconductor device that is sensitive to infrared radiation. When infrared radiation strikes the sensor, it generates an electrical signal proportional to the intensity of the radiation.

Infrared cameras may use various types of sensors, including [17]:

1. Thermal imaging sensors: These sensors detect long-wave infrared radiation (also known as thermal radiation) emitted by objects. They are typically based on materials such as vanadium oxide (VOx) or amorphous silicon (a-Si). Thermal imaging sensors can detect minute temperature differences and produce images based on these variations.
2. Infrared detectors: These sensors detect both short-wave and long-wave infrared radiation. They are often used in applications such as night vision, where they can detect infrared light emitted by objects or reflected from surfaces.

Once the sensor detects the infrared radiation, the camera processes the electrical signals to create a visual representation of the scene. This process is known as thermography or thermal imaging. The camera assigns different colors or shades to different temperature levels, allowing users to visualize temperature variations in the scene.

Infrared cameras have various applications across industries, including [14]:

- Building inspections: Identifying areas of heat loss or moisture intrusion in buildings.
- Electromechanical inspections: Detecting overheating components in electromechanical systems.
- Industrial monitoring: Monitoring temperature levels in manufacturing processes.

- Medical imaging: Detecting abnormalities in the human body based on temperature variations.

Overall, the principle of an infrared camera involves detecting infrared radiation emitted by objects and converting it into a visible image based on temperature differences, enabling users to identify patterns or anomalies that are not visible to the naked eye.

2.5.4 Domain of use of infrared thermography

Temperature is a very reliable characteristic that uses thermal data to reveal information about equipment condition and to provide insights into thermal distribution. Infrared Thermography is primarily used in preventive maintenance, condition monitoring, inspections, and fault diagnostics. The next part will explore the wide range of sectors in which infrared thermography finds application.

2.5.4.1 Medical Applications

Variations in body temperature are accurate markers of disease. In this situation, Infrared Thermography (IRT) is a non-invasive, non-contact method for taking a person's body temperature remotely. When it comes to the field of cancer detection, aberrant heat patterns are produced in the afflicted area when cancer cells are present. A tumor's presence causes increased blood flow and metabolic rates, which raise body warmth and indicate the presence of malignancy.

Variations in the skin's surface temperature can be used to diagnose diabetic neuropathy and vascular diseases. Inflammatory skin illnesses show up as irregular temperature patterns on the skin's surface. When it comes to identifying a range of medical ailments, such as fever screening, skin infections, heart difficulties, gynecological disorders, and brain imaging, Infrared Thermography (IRT) has shown to be highly adaptable. Thermal cameras are useful for diagnosing kidney and liver problems as well as early warning signs of heart attacks. Since early disease diagnosis via IRT can greatly assist in treatment and even save lives, its implementation in a variety of contexts becomes imperative [21].

2.5.4.2 Gas Detection

A number of chemical substances and gases are imperceptible to the unaided sight, and some of these may be dangerous or toxic air pollutants. Pipes and valves are frequently used to convey gasses and chemical compounds released from sources such as petrochemical facilities and oil refineries. Here, Infrared Thermography (IRT) offers a wealth of data regarding the state of insulation in pipes, tubes, and valves. Facilities like petrochemical plants may have a lot of leak locations. Because they can record specific infrared wavelengths, thermal cameras are helpful in the detection of gas leaks. If gas is present, the corresponding area appears dark when radiation from these bands is absorbed by it.

Leaks can be seen as smoke on the camera screen thanks to the visual representation of the equipment's state provided by the camera. This enables real-time gas detection and helps users detect the presence of hazardous chemicals. Without coming into contact with dangerous substances directly, inspectors can safely detect gas leaks by using Infrared Thermography (IRT). Particles of volcanic ash can also be found using infrared cameras [22].

2.5.4.3 Agriculture

Infrared Thermography (IRT) has several uses in the food and agricultural industries [23]. An irrigation schedule can be made easier and soil water levels can be predicted with the use of a thermal camera. Temperature rises on the leaf surface act as markers of the growth of infections, and IRT is useful in the detection of pathogens and illnesses. Because injured fruits have lower temperatures than unbruised ones, thermal cameras are useful for spotting fruit bruises, evaluating fruit maturity times, and estimating fruit production. Moreover, IRT is used to find foreign particles in fruits and vegetables. For this, the differences in emissivity and heat capacity between the fruit itself and the foreign particles are used. This technique, which locates moist regions, is also helpful for storing grains.

2.5.4.4 Aviation

Infrared Thermography (IRT) is a useful tool in the field of aviation safety and security. Thermal cameras are employed in the inspection of various aircraft parts, allowing for the prompt and highly accurate detection of flaws. Moreover, thermal cameras can be installed on an aircraft's front lower side to give pilots important information about the outside weather. By improving the pilot's eyesight and making them aware of the circumstances, these cameras help make airplane landings safer at night, in fog, and in the rain [24].

2.5.4.5 Animals

Animals with warm blood try to keep their bodies at a constant temperature in reaction to their surroundings [25]. The body's uneven temperature distribution is a result of breathing and blood circulation. Animals can be used to identify hot and cold regions on their bodies by using a thermal camera. Veterinarians can use this knowledge to anticipate problems with veins, skin, and joints without having needless procedures performed.

Infrared Thermography (IRT) is a diagnostic technology used in veterinary care to identify specific diseases in animals. There is an increase in temperature in the gluteal regions of sick dairy animals. A horse's body may have hotspots that represent inflammation or enhanced blood flow and cold areas that represent edema or scar tissue. Thermal cameras are helpful for tracking animals in woods at night since they can function in total darkness.

2.6 Diagnosis by infrared thermography

The principle of faults diagnosis in electromechanical systems through thermography involves utilizing infrared imaging to detect temperature variations in the targeted object. This diagnostic method relies on the fact that different faults or abnormalities, such as overheating due to electrical faults, friction, or insulation breakdown, result in temperature changes that can be detected by an infrared camera.

Infrared thermography is an imaging technique that allows temperature variations to be visualized on a surface using a thermal camera. This technology uses infrared radiation emitted by objects to create a thermal image [14].

In the field of industry thermographic diagnostics is the process of inspecting electromechanical systems using infrared thermography to detect hot spots or thermal anomalies that could indicate potential problems. Common defects detected by thermography include, for example [17].

1. Winding overheating: Insulation breakdown or overload conditions can cause excessive heat in the machine windings, which can be detected as hot spots in thermographic images.

2. Bearing Problems: Failing bearings often generate heat due to increased friction or lack of lubrication. Thermography can identify overheating bearings before they fail.

3. Imbalance or Misalignment: Misaligned or unbalanced components can cause uneven loading and friction, resulting in localized heating that can be detected by thermography.

4. Electrical faults: Loose connections, damaged cables or faulty electrical components can lead to resistive heating and hot spots in machines.

2.6.1 Operating principle

When an electromechanical system operates normally, it produces heat uniformly. However, in the event of a malfunction, such as overloading or a poor connection, some parts of the equipment may become hotter than others. Infrared thermography makes it possible to detect these temperature variations and identify problem areas.

2.6.2 Analysis of results

Once thermal images are captured, they are analyzed to identify the existing anomalies. This analysis can be performed by comparing measured temperatures to reference values, using industry standards or predefined thresholds to determine if corrective action is necessary.

2.6.3 Preventive Maintenance

Infrared thermography is often used as part of preventive maintenance programs to identify and correct potential problems before they become critical, reducing the risk of costly breakdowns and unplanned downtime.

The principle of electromechanical systems faults diagnosis by thermography is to use infrared thermography technology to detect abnormal temperature alteration from a predefined set point, thereby identifying potential problems and taking corrective action before they cause damage or service interruptions. The early detection of these temperature anomalies, helps maintenance personnel to take corrective action to avoid further damages or breakdowns, minimize downtime and extend the life of electromechanical equipment.

2.7 State of the Art of Diagnostics using Thermography

Temperature is a reliable physical quantity which when it is accurately measured, provides information about the target's thermal distribution. This acquired thermal data is then used to reveal information about the condition of the equipment. Basically, condition monitoring, inspections, fault detection and preventive maintenance are carried out via infrared thermography (IRT) in a large interval of industries. In this section we will explore the uses of this technique in a number of recently published works related to the diagnosis of defects in electromechanical systems.

Many research projects have been published in well rated journals. The amount of research has increased significantly over time, and some work has been presented to show the variety of approaches and areas of focus used in these efforts [26,35].

Certainly, here are some recent references that discuss the state of the art in infrared thermography applied to electromechanical equipment:

- **"Infrared Thermography for Monitoring and Fault Diagnosis of Electromechanical Systems: A Review"**

Zhang, Y. et al [26], in this review article, provides an overview of infrared thermography applications for monitoring and fault diagnosis of electromechanical systems. It covers topics such as fault detection algorithms, image processing techniques, and case studies in various industrial applications.

- **"Recent Advances in Infrared Thermography for Condition Monitoring and Fault Diagnosis of Electromechanical Systems"**

Li, W., et al. [27], discusses in this paper recent advances in infrared thermography for condition monitoring and fault diagnosis of electromechanical systems. It reviews state-of-the-art techniques for data analysis, anomaly detection, and predictive maintenance, with a focus on practical applications.

- **"Application of Infrared Thermography in Diagnosis and Fault Analysis of Electromechanical Systems: A Review"**

Sun, X., et al. [28], in this review article, provides a comprehensive overview of the application of infrared thermography in the diagnosis and fault analysis of electromechanical systems. It discusses recent developments in thermal imaging technology, image processing algorithms, and case studies in different industrial sectors.

- **"State-of-the-Art Review on Infrared Thermography for Condition Monitoring and Fault Diagnosis of Electromechanical Systems"**

Yu, D., et al. [29], presents a state-of-the-art review on the application of infrared thermography for condition monitoring and fault diagnosis of electromechanical systems. It discusses recent advancements in thermographic imaging technology, signal processing methods, and case studies in various applications.

- **"Recent Advances in Infrared Thermography for Condition Monitoring and Fault Diagnosis of Electrical and Electromechanical Equipment"**

Wang, Z., et al. [30], *in* this review paper provides an overview of recent advances in infrared thermography for condition monitoring and fault diagnosis of electrical and electromechanical equipment. It covers topics such as data analysis techniques, fault detection algorithms, and case studies in different industrial settings.

- **"Recent Advances in Infrared Thermography for Fault Diagnosis of Electromechanical Equipment: A Review"**

Zhou, S., et al. [31], reviews recent advances in infrared thermography for fault diagnosis of electromechanical equipment. It covers topics such as machine learning techniques, deep learning algorithms, and case studies in different industrial applications.

- **"Advances in Infrared Thermography for Condition Monitoring and Fault Diagnosis of Electromechanical Systems: A Review"**

Li, H., et al. [32], in this review article provides an overview of advances in infrared thermography for condition monitoring and fault diagnosis of electromechanical systems. It discusses recent developments in image processing, feature extraction, and fault detection methods.

- **"Infrared Thermography for Condition Monitoring and Fault Diagnosis of Electromechanical Systems: Recent Advances and Future Directions"**

Liu, J., et al. [33], discusses recent advances and future directions in infrared thermography for condition monitoring and fault diagnosis of electromechanical systems. It reviews emerging technologies, challenges, and opportunities in the field.

- **"Recent Progress in Infrared Thermography for Fault Diagnosis of Electromechanical Equipment: A Review"**

Chen, Y., et al. [34], in this review paper provides an overview of recent progress in infrared thermography for fault diagnosis of electromechanical equipment. It discusses advancements in thermal imaging technology, data analysis techniques, and case studies in different industrial sectors.

- **"Application of Infrared Thermography in Condition Monitoring and Fault Diagnosis of Electromechanical Equipment: A Review"**

Chen, H., et al. [35], presents an overview of the application of infrared thermography in condition monitoring and fault diagnosis of electromechanical equipment. It covers recent developments in thermal imaging technology, image processing methods, and case studies in various industries.

These references offer a comprehensive overview of the current state of the art in infrared thermography as applied to electromechanical equipment, covering recent advancements, challenges, and applications.

2.8 Advantages and Limitations in diagnosis using thermography

The use of infrared thermography offers several advantages [14], including:

- **Non-Contact Measurement:** Infrared thermography enables remote temperature measurement without the need for physical contact with the object under inspection.
- **Rapid Inspection:** Thermal imaging allows for rapid and comprehensive inspections of large areas or complex structures.
- **Early Detection of Anomalies:** Infrared thermography can detect subtle temperature variations indicative of defects or abnormalities, enabling early intervention and preventive maintenance.

However, infrared thermography also has limitations [19], including:

- **Surface Sensitivity**: Infrared thermography primarily measures surface temperatures and may not accurately assess temperatures within the bulk of materials or objects.

- **Environmental Factors:** Environmental conditions such as ambient temperature, humidity, and air movement can affect the accuracy and interpretation of thermal images.
- **Equipment and Expertise Requirements:** Effective implementation of infrared thermography requires specialized equipment, trained personnel, and expertise in data interpretation and analysis.

To overcome these limitations, in this thesis we propose the use of machine learning techniques combined with infrared thermography (IRT); which are detailed in a clearer and a more explained fashion in the chapters that follow.

Using machine learning methods on thermal images analysis offers many advantages over traditional methods that rely solely on thermal data, including:

1. Automated Flaw Detection: Machine learning algorithms that can automatically identify patterns and anomalies in thermographic data without the need for manual interpretation. This automation streamlines the analysis process and enables rapid detection of defects in electromechanical systems.

2. Improved accuracy: Machine learning models can learn complex patterns and relationships in thermographic data, leading to more accurate defect detection compared to manual or rules-based approaches. These models can handle large data sets and extract subtle features that may not be apparent to human analysts.

3. Improved predictive capability: Machine learning techniques enable predictive maintenance by identifying early indicators of engine degradation or failure in thermographic images. By analyzing historical data and learning from past patterns, these models can predict potential issues before they become serious, minimizing downtime and maintenance costs.

4. Adaptability to various conditions: Machine learning algorithms are robust and adaptable to various operating conditions, environmental factors and machine configurations. They can generalize well to new datasets and environments, making them suitable for real-world applications in different industries and systems.

Overall, leveraging machine learning methods for thermographic analysis offers a more efficient, accurate, and scalable approach to electromechanical systems faults diagnosis, enabling proactive maintenance and minimizing unplanned downtime.

2.9 Conclusion

Due to its high speed, purity, and safety, infrared thermography is widely used in many different fields. Its application in containing two critical areas temperature measurement and non-destructive testing has been examined in this chapter. These fields have had their fundamental ideas and theoretical foundations scrutinized. This prior knowledge helps to understand these technologies better and offers insightful information. Recent developments in these fields have also been examined and explained.

Rapidly, infrared thermography has advanced significantly in a number of fields. Even with these advancements, a few restrictions need to be carefully considered. The choice of sensor and experimental design have a significant impact on the effectiveness of infrared thermography, and these factors are influenced by the surroundings as well as the device. In order to mitigate these issues, careful setup and testing protocols are necessary, which heavily depend on the operator's experience.

Chapter 3: Image processing and features extraction

3.1 Introduction

Image processing is a method used to perform operations on an image to improve it or extract useful information. It is a type of signal processing in which the input is an image, such as a photograph or video frame, and the output can be either an image or a set of characteristics or parameters related to the image. The involved processes can range from simple tasks such as scaling and rotation to more complex operations such as image segmentation, pattern recognition and feature extraction.

The use of different algorithms and methods to digitally alter and examine photos is known as image processing. This entails using mathematical transformations and operations to improve image quality, retrieve useful data, or complete particular tasks.

Understanding the fundamental definition of an image is crucial in the fields of image processing and computer vision. An image is a visual representation of an object, scene, or phenomenon captured through a variety of means such as photography, scanning, or digital rendering.

3.2 Definition of an Image

3.2.1 Basic Definition

An image can be defined as a two-dimensional array of values, typically representing light intensity or color information. These values, known as pixels, form the smallest unit of an image and collectively define the image's appearance [36].

- **Pixel**: Short for "picture element," a pixel is the smallest addressable element in a digital image. Each pixel has a specific value that represents its color or intensity.

3.2.2 Types of Images

Images can be classified based on various criteria, including their origin, dimensionality, and the type of information they contain [37].

3.2.2.1 Raster Images

Raster images, also known as bitmap images, are composed of a grid of pixels. Each pixel has a specific color or intensity value, and the image's resolution is defined by the total number of pixels along its width and height. The primary characteristics of raster images include resolution and color depth.

- **Resolution**: The number of pixels in an image, typically represented as width x height (e.g., 1920x1080). Higher resolution images contain more detail.
- **Color Depth**: The number of bits used to represent the color of each pixel. Common color depths include 8-bit (256 colors), 24-bit (16.7 million colors).

3.2.2.2 Grayscale Images

Grayscale images represent intensity information using shades of gray, without any color information. Each pixel in a grayscale image has an intensity value ranging from black to white.

- **Bit Depth**: Common bit depths for grayscale images include 8-bit (256 levels of gray) and 16-bit (65 536 levels of gray).

3.2.2.3 Binary Images

Binary images, also known as bi-level or two-level images, consist of pixels that can have only one of two possible values, typically black or white. These images are often used for simple graphics, text representation, and some types of image analysis.

- **Bit Depth**: Binary images have a bit depth of 1, meaning each pixel is represented by a single bit (0 for black and 1 for white)

3.2.2.4 Color Images

Color images contain information about the color of each pixel. The most common color model used is the RGB model, where each pixel is defined by its red, green, and blue components.

- **RGB Model**: A color model where colors are represented by their red, green, and blue components. Other models include CMYK (used in printing) and HSV (hue, saturation, value).

3.2.2.5 3D Images

3D images represent objects in three dimensions, providing depth information in addition to the usual two-dimensional spatial information. These images can be created using various techniques, including stereoscopic imaging, laser scanning, and computed tomography (CT).

- **Voxel**: The three-dimensional equivalent of a pixel, representing a value in a 3D space.

3.2.2.6 Thermal Images

Thermal images capture infrared radiation, which is emitted by objects based on their temperature. These images are used in applications such as industrial monitoring night vision, medical diagnostics, and building inspections.

- **Infrared Imaging**: The technique used to capture thermal images, sensitive to the infrared portion of the electromagnetic spectrum.

3.2.2.7 Medical Imaging

Medical imaging encompasses various techniques to visualize the interior of the body for clinical analysis and medical intervention.

- **X-ray**: Uses X-rays to view inside the body, especially useful for examining bones.

- **MRI (Magnetic Resonance Imaging)**: Uses strong magnetic fields and radio waves to generate detailed images of organs and tissues.
- **CT (Computed Tomography)**: Combines X-ray measurements from different angles to create cross-sectional images.
- **Ultrasound**: Uses high-frequency sound waves to capture live images from the inside of the body.

The definition of an image encompasses a broad range of types, formats, and characteristics. From the fundamental pixel-based raster images to scalable vector graphics. Each type of image has its unique properties and applications. Understanding these basics is essential for effectively working with images in various fields, including digital art, photography, medical imaging, and computer vision. As technology evolves, the methods for capturing, storing, and processing images continue to advance, expanding the possibilities for visual representation and analysis.

3.3 Image Processing

Imaging devices such as cameras can take pictures by using sensors that provide an analog signal. A digital image is then produced by digitizing this analog signal [38].

3.3.1 Preprocessing

Preprocessing steps are essential to prepare the image for further analysis by enhancing its quality and removing artifacts.

- **Noise Reduction**: Images often contain noise due to sensor errors or environmental conditions. Techniques such as Gaussian filtering, median filtering, and bilateral filtering are used to reduce noise while preserving edges.
- **Contrast Enhancement**: Methods like histogram equalization, adaptive histogram equalization (CLAHE), and contrast stretching improve the visibility of features in an image, making it easier to analyze.
- **Normalization**: This process adjusts the range of pixel intensity values to a standard scale, which helps in consistent analysis across different images.

3.3.2 Image Transformation

Image transformation techniques are employed to change the representation of the image, facilitating specific types of analysis.

- **Fourier Transform**: This mathematical transformation converts an image from the spatial domain to the frequency domain, helping to analyze periodic patterns and filter out noise.
- **Wavelet Transform**: Unlike the Fourier transform, which provides frequency information, the wavelet transform offers both spatial and frequency information, making it useful for multi-resolution analysis.

3.3.3 Image Segmentation

Segmentation divides an image into distinct regions or objects for easier analysis.

- **Thresholding**: A simple method that separates objects from the background based on pixel intensity. Otsu's method is a popular approach for automatic threshold selection.
- **Edge Detection**: Techniques like the Canny, Sobel, and Prewitt detectors highlight the boundaries of objects by identifying points where the image intensity changes sharply.
- **Region-Based Segmentation**: Methods such as region growing, watershed algorithm, and k-means clustering segment an image based on the similarity of pixels in terms of intensity, color, or texture.

3.4 Image feature extraction

Feature extraction is crucial for identifying and isolating various attributes or shapes within an image, which are essential for tasks such as object recognition and classification [39].

3.4.1 Keypoint Detection

Keypoint detection identifies significant points in an image that can be used for further analysis.

- **SIFT (Scale-Invariant Feature Transform)**: This algorithm detects and describes local features in images, providing invariance to scale and rotation. It is widely used for object recognition and image stitching.
- **SURF (Speeded Up Robust Features)**: An optimized version of SIFT, SURF is faster and more robust, making it suitable for real-time applications.

3.4.2 Corner Detection

Corner detection identifies points in an image where the curvature is high, often corresponding to significant structural features.

- **Harris Corner Detector**: This algorithm measures the local changes in intensity in multiple directions, identifying corners with high precision.
- **FAST (Features from Accelerated Segment Test)**: A high-speed corner detection method often used in real-time applications like mobile robotics.

3.4.3 Blob Detection

Blob detection methods identify regions in an image that differ in properties such as brightness or color from surrounding regions.

- **Laplacian of Gaussian (LoG)**: This method detects blobs by finding the maxima and minima in the Laplacian of the image.
- **Difference of Gaussians (DoG)**: An approximation of LoG, DoG is computationally efficient and widely used in computer vision.

3.4.4 Edge Features

Edges represent significant changes in intensity in an image and are fundamental for object boundary detection.

- **Canny Edge Detector**: A multi-stage algorithm that provides robust edge detection by applying Gaussian filtering, finding intensity gradients, and applying non-maximum suppression.
- **Sobel and Prewitt Operators**: Simple gradient-based methods that highlight edges by calculating the intensity gradient in the image.

3.5 Types of image descriptors

Depending on the needs of the application, the features that are retrieved from photos can be divided into two categories: local and global features. Local features are used for more complex applications like object recognition, while global features are usually used for low-level tasks like item detection and classification [40].

3.5.1 Local Descriptors

Local descriptors focus on capturing information from specific parts of an image, usually around keypoints or interest points. They are designed to be robust to variations in viewpoint, scale, and illumination.

Examples and Definitions:

1. **SIFT (Scale-Invariant Feature Transform)**:

   - **Definition**: SIFT detects and describes local features by identifying keypoints and computing descriptors that are invariant to scale and rotation.
   - **Application**: Used in object recognition, image stitching, and 3D reconstruction.

2. **SURF (Speeded-Up Robust Features)**:

   - **Definition**: SURF is a faster alternative to SIFT, using a Hessian matrix-based approach for keypoint detection and descriptors based on Haar wavelet responses.
   - **Application**: Suitable for real-time applications due to its speed.

3. **ORB (Oriented FAST and Rotated BRIEF)**:

- **Definition**: ORB combines the FAST keypoint detector with the BRIEF descriptor, adding orientation information to make the descriptors rotation invariant.
- **Application**: Commonly used in mobile and embedded systems for its efficiency.

4. **HOG (Histogram of Oriented Gradients)**:

- **Definition**: HOG descriptors capture edge and gradient information by computing histograms of gradient orientations within localized regions of an image.
- **Application**: Widely used in human detection and other object recognition tasks.

3.5.2 Global Descriptors

Global descriptors capture information from the entire image, providing a holistic representation. These descriptors are typically used for image retrieval, classification, and overall scene understanding.

Examples and Definitions:

1. **Color Histograms**:

- **Definition**: A color histogram represents the distribution of colors in an entire image by counting the number of pixels for each color or color range.
- **Application**: Used in image retrieval and indexing based on color content.

2. **GIST Descriptor**:

- **Definition**: The GIST descriptor captures the spatial layout and structure of an image by applying a set of Gabor filters at different scales and orientations.
- **Application**: Used for scene classification and image retrieval.

3. **Edge Histogram Descriptor (EHD)**:

- **Definition**: EHD captures the global distribution of edges in an image by dividing the image into sub-blocks and computing histograms of edge directions within each block.
- **Application**: Used in image retrieval and classification based on edge information.

Both local and global descriptors play essential roles in image applications and computer vision, each serving different purposes depending on the application's requirements. Local descriptors excel in tasks requiring precise matching and recognition of image parts, while global descriptors provide a comprehensive overview useful for classification and retrieval. Understanding their differences and applications allows for more effective utilization in various visual analysis tasks.

3.6 Features extraction methods

Feature extraction methods are essential for analyzing and understanding images in computer vision. Each method has unique strengths and applications, from object detection and recognition to texture analysis and image compression. Choosing the appropriate feature extraction method depends on the specific requirements of the task at hand, such as the need for real-time processing, the strength of transformations, or capturing specific types of image information.

Below we will provide a detailed explanation of the feature extraction methods that we will use in diagnosing electromechanical systems.

3.6.1 Image Features extraction using Bag of Visual Words (BoVW)

The incredible performance of "Bag-of-Words" (BoW) in text retrieval has made it possible for its use as a dependable feature extraction technique across a range of applications. It is known as "Bag-of-Visual-Words" (BoVW) in image processing. Like BoW, BoVW converts a picture into a histogram, which is essentially a representation of the visual characteristics of the processed image. According to Zhen et al. [37], this histogram is a useful feature store for later picture categorization. The two steps listed below are used to derive the BoVW method:

Step 1: Visual words extraction method

Several methods have been used to extract visual words from regions of interest in infrared thermography images, using techniques for local feature identification and description. Local feature descriptors effectively define a pixel's representation in an image by encapsulating its local information. To identify equivalent pixel positions in images that transmit similar quantitative information about spatial intensity patterns in different states or modes, these descriptors need to be highly resilient against localization mistakes and deformations.

We give a brief description and comparison of the Scale Invariant Feature Transform (SIFT) and Speeded Up Robust Feature (SURF) local feature extraction techniques in the paragraph that follows.

1. Scale Invariant Feature Transform (SIFT)

The Scale Invariant Feature Transform (SIFT) approach was first presented by David et al. in 2004. It uses a 128-dimensional vector called the SIFT descriptor. This descriptor captures gradients from 4x4 places surrounding a pixel and is stored in a histogram with eight major orientations. Scale invariance is obtained by vector computing in various Gaussian scale spaces, whereas rotation invariance is obtained by aligning the gradients with the primary direction. It is important to remember that in some implementations, like facial recognition, invariant rotation descriptors can result in false matches. The alignment of the descriptor gradients can point in a certain direction if rotation invariance is not required.

The difference of the Gaussian function scale-space extreme is used to discover and locate stable locations of interest points in a scale space, which is important [33]. The scale space can be described as follows: It is the result of convolutioning the original image with a variable scale Gaussian function.

$$L(\rho,\sigma) = G(\rho,\sigma) * I(\rho) \qquad (3.1)$$

Where $*$ is the convolution operator and $\rho = (x, y)$ is a point in the IRT image.

The Gaussian function G (ρ, σ) is defined as:

$$G(\rho,\sigma)=\frac{1}{2\pi\sigma^2}e^{\left(\frac{-(x^2+y^2)}{2\sigma^2}\right)} \qquad (3.2)$$

The scale-space extreme convolution with D(ρ, σ) allows for the differentiation of two scales via a multiplicative index k, which can be written as follows:

$$D(\rho,\sigma)=\big(G\ (\rho,k\sigma)\ -\ G(\rho,\sigma)\big)*I(\rho)$$

$$=L(\rho,k\sigma)-L(\rho,\sigma) \qquad (3.3)$$

While * represents the convolution product.

By carefully localizing the interest points using the suggested technique, which is referred to as the Taylor expansion of the scale-space function D(ρ, σ), as shown in Equation (4.4), it is possible to identify the local extremes of the function D.

$$D(\rho,\sigma)=D+\frac{\partial D^T}{\partial\rho}\rho+\frac{1}{2}\rho^T\frac{\partial^2 D}{\partial^2\rho}\rho \qquad (3.4)$$

2. Speeded Up Robust feature (SURF)

First presented by Bay et al. in 2008, the SURF algorithm is a ground-breaking technique for identifying and characterizing rotation- and scale-invariant interest sites. For every image, it generates a set of interest points and a set of 128-dimensional descriptors for every point.

The SURF descriptor is conceptually similar to SIFT, but it also concentrates on the gradient information that is dispersed throughout the space around the interest point. Using its detection techniques or in a regular grid, the interest point itself can be localized and described. Rotation, scale, brightness, and, if normalized to unit length, contrast are all invariant to SURF. Due to this property, SURF computation can be completed quickly while yet being resilient against rotation within a range of approximately ± 15°, which is common for many face recognition tasks. When handling different picture perturbations, SURF descriptors are known to be more robust than locally functioning SIFT descriptors.

The localization of SURF detector interest points is based on the Hessian matrix.If a point $\rho = (x, y)$ in an IRT image *I*, is considered then, the Hessian matrix $H = (\rho, \sigma)$ at ρ and scale σ is expressed as follows:

$$H = (\rho, \sigma) = \begin{bmatrix} L_{xx}(\rho, \sigma) & L_{xy}(\rho, \sigma) \\ L_{xy}(\rho, \sigma) & L_{yy}(\rho, \sigma) \end{bmatrix} \quad (3.5)$$

While $L_{xx}(\rho, \sigma)$ is the second order derivative of the Gaussian convolution $\frac{\partial^2}{\partial x^2} G(\rho, \sigma)$ with the image I , and likewise for $L_{xy}(\rho, \sigma)$ and $L_{yy}(\rho, \sigma)$.

SURF uses average box filters to approximate second-order Gaussian derivatives in a close-to-approximate manner. SIFT, on the other hand, uses the Gaussian difference (DoG) to approximate the Gaussian Laplacian (LoG) more closely. Integral images provide quick computation in SURF, as demonstrated in Figure 1. By calculating the Hessian matrix determinant, the position and scale of the interest point can be chosen. It then applies non-maximum suppression in a 3×3×3 neighborhood to localize the interest points in picture space and scale.

By creating a circular zone around the identified interest point and designating a distinct orientation, the SURF descriptor is created. In order to provide invariance to picture rotations, the orientation is determined using the Haar wavelet response in both the x and y dimensions. Integral pictures are used to efficiently calculate Haar wavelets.

Once the dominant orientation has been established, the square areas surrounding the interest spots are extracted and included into the SURF descriptors. Each sub-region is partitioned into 4x4 segments, and the underlying intensity pattern (first derivatives) of each window is represented by a vector V.

$$V = \left[\sum \partial_x , \sum \partial_y , \sum | \partial_x |, \sum | \partial_y | \right] \quad (3.6)$$

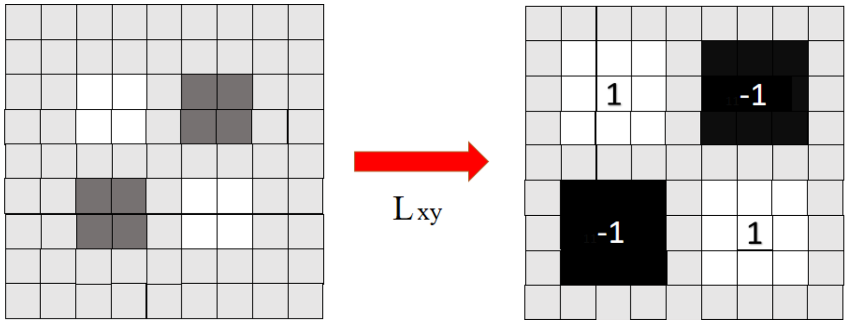

Figure 3.1: Second order partial derivatives of the Gaussian function and its corresponding box filter.

Ultimately, there are four main steps that make up the SURF method:

a. From the input image, create the integral image by summing the pixels over the portions that are rectangular and upright.

b. Create the Hessian response map determinant, which will produce a localized interest point vector by using non-maximal suppression to localize scale space interest points. In this stage, the Hessian Matrix determinant is used.

c. Determine the interest points' main direction and build a 4x4 window around their neighborhood. Utilizing the sums of the Haar wavelet responses from every sub-region, create a 128-dimensional descriptor vector.

d. Store the relevant information for every site of interest.

One of the main benefits of the SURF descriptor is thought to be its ability to compute distinctive descriptors quickly. It is also a dependable option for this work due to its invariance to common image modifications such image rotation, scale, illumination changes, and slight viewpoint adjustments. It is justified, in light of the information previously provided, to use the SURF approach as the feature extractor in our experimental study.

Step 2: Histogram of SURF features

A histogram that shows the frequency of recurrence of these visual words is created from the encoded features. k-means clustering is used before feature encoding to provide a lexicon, or numerous interest points.

A specified vocabulary size can be obtained by clustering each faulty state extracted features and a set of k clusters is learned. After that, the centers of the learned clusters are defined as the vocabulary. In this paper, a set of *n* dimensional vectors of SUFT features ($x1$, $x2$,…, xn) is done. Via k-means clustering, the *n* SUFT vectors are divided into k different groups such that $S = \{S1, S2, \ldots, Sk\}$ with minimized intracluster squared summed error (SSE), which is done as:

The attributes taken out of each defective condition are clustered to produce a collection of k clusters, which in turn determine a certain vocabulary size. The defined vocabulary is formed by the centers of these clusters. A set of n-dimensional vectors of SURF features ($x1$, $x2$,…, xn) is taken into consideration in this study. The n SURF vectors are divided into k different groups using k-means clustering; these groups are represented as $S = \{S_1, S_2, \ldots, Sk\}$, with the goal of minimizing the intracluster squared summed error (SSE) as follows:

$$S = \arg\min_s \sum_{i}^{k} \sum_{x \in s_i} \lVert x - u_i \rVert^2 \qquad (3.7)$$

Where are the mean vector in .

3.6.2 Image features extraction using GIST method

The GIST can be computed as a single feature vector when our data is treated as an image [38], providing a complete picture representation. Originally created for image classification tasks, thirty-two (32) feature maps with the same resolution as the original picture are produced by convolving an image with thirty-two (32) different Gabor filters at eight (08) directions and four (04) scales. This process determines the GIST of an image. Each feature map is then partitioned into 16 regions using a 4x4 grid, and the average values are calculated for each region. The GIST is meant to provide a concise summary of gradient information about sizes and orientations in different areas of an image. At the end, each image is converted into a 2048-dimensional feature vector by multiplying 32 feature maps by 16 (4x4) regions.

There are multiple steps in the GIST processing. The data (picture) is first divided into several blocks or areas, and Gabor filters with different sizes and orientations are applied to each block. The final features are then calculated by averaging over various regions. This block split improves feature accuracy and guards against information loss. The following is an outline of the process: First step: Apply convolution to the image's various sections one after the other.

Second step: In order to determine the image's global GIST feature, the findings must be combined in the second phase. The resulting matrix is split into k_a×k_a blocks if the source image is processed with a size of M×N. Every block, where i=1,...,k_a, is considered a region and is represented as B_a. In order to optimize calculation and processing, each block has the identical Mʊ × N′ dimensions. Using k_g= k_a× k_a, the blocks' global information is kept.

In the third stage, the image's component blocks are labeled and given the B_a tag. To make computation easier, every block is the same size, measuring Mʊ × N′. In order to achieve the self-similarity of the Gabor filter and variant Gabor filters, the mother wavelet filter is generated by a series of transformations and mathematical procedures. The Gabor filter's mother wavelet can be stated as follows:

$$g(x,y) = \frac{1}{2\pi\sigma_x\sigma_y}\exp[\,\text{-}\,(\frac{x^2}{\sigma_x^2} + \frac{y^2}{\sigma_y^2})] \times \cos(2\pi f_0\, x + \varphi) \qquad (3.8)$$

The formula's variables x and y stand for the pixel's positional data. The Gaussian standard deviation along the x- and y-axes is shown by the symbols σ_x and σ_y, respectively. The phase shift is denoted by φ, while the center frequency is represented by f_0. A collection of Gabor filters in various sizes and directions can be used to mathematically represent the mother wavelet. The exact formula is as follows:

$$\begin{cases} g_{mn}(x,y) = a^{-m} g(x',y'), \quad a > 1 \\ x' = a^{-m}(x \cos\theta + y \sin\theta) \\ y' = a^{-m}(-x \sin\theta + y \cos\theta) \\ \theta = \frac{n\pi}{n+1} \end{cases} \tag{3.9}$$

The scale factor is written as a^{-m}, where n is the number of directions, m is the number of scales, and θ is the rotation angle. After the computation, m × n Gabor filters ought to be acquired. The cascade procedure is then introduced after a comparable operation has been applied to various areas of the original image. The image's final GIST characteristic is expressed as follows:

$$V_i^B(x,y) = cat\left(I(x,y) * g_{mn}(x,y)\right), (x,y) \in B_i \tag{3.10}$$

V^B is the block GIST feature.

The global GIST feature of the image is created by averaging the block GIST features acquired for each filter and integrating the resulting rows:

$V_G = \left\{\overline{V_1^B}, \overline{V_2^B}, \ldots\ldots, \overline{V_{n_g}^B}\right\}$, V_G represents the global GIST feature, and $\overline{V_\iota^B}$ is the mean of the block GIST feature.

$\overline{V_\iota^B}$ is calculated as follows:

$$\overline{V_\iota^B} = \frac{1}{M' \times N'} \sum_{(x,y) \in B_i} V_I^B(x,y) \tag{3.12}$$

In this thisis, V_G represents the global feature of image.

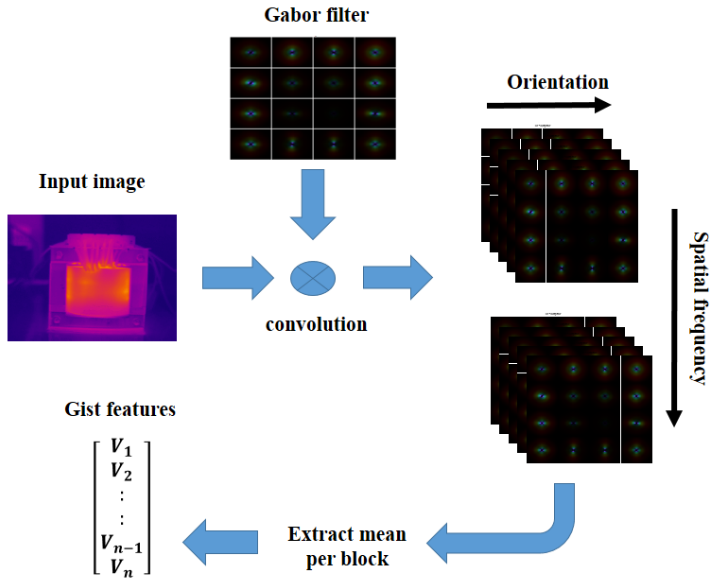

Figure 3.2 GIST feature extraction steps

3.7 conclusion

In this chapter, we have explored the fundamental concepts and techniques involved in image processing and feature extraction. Image processing provides the essential tools and methods for manipulating and analyzing digital images, enabling a wide range of applications from medical imaging to computer vision.

We began by discussing the different types of images, including raster and grayscale color images and thermal images, as well as specialized formats like multispectral and hyperspectral images. Understanding these types and their characteristics is crucial for selecting appropriate processing techniques and achieving desired outcomes.

We then delved into the concept of image features, which are critical for understanding and interpreting visual information. Features can be broadly categorized into local and global descriptors. Local descriptors, such as SIFT, SURF, ORB, and HOG, focus on capturing detailed information around keypoints or interest points, making them robust to changes in scale, rotation, and partial occlusion. These descriptors are indispensable for tasks like object recognition, image matching.

On the other hand, local and global descriptors, including BoVW, GIST provide a holistic representation of an image, capturing overall characteristics and patterns. These descriptors are particularly useful for image retrieval, classification, and scene understanding, offering a summarized view of the image content.

Building upon the aforementioned feature extraction techniques, the results obtained during the extraction phase serve as critical inputs for artificial intelligence classifiers. These classifiers are employed in the context of fault diagnosis for electromechanical systems. By accurately extracting relevant features from the data, we can enhance the performance and accuracy of these AI classifiers, enabling them to identify and diagnose faults more effectively.

Chapter 4: Machine learning and classification

4.1 Introduction

Significant advances in computer science and technology in the late 20th century cleared the way for the emergence of a new paradigm centred on artificial intelligence. This paradigm made it possible to create intelligent machines that mimic human intelligence and have the capacity for learning, decision-making, and outcome prediction. Applications for artificial intelligence can be found in many fields, such as industrial equipment monitoring and diagnosis.

The goal of this chapter is to define artificial intelligence and its uses, with a particular emphasis on machine learning, a field that is essential to our work.

4.2 Artificial intelligence

Artificial intelligence, or AI, is the study of calculations that enable robots to mimic human perception, reasoning, and behavior. Artificial Intelligence (AI) refers to machines that have been programmed to mimic human thought processes and behavior. Any machine exhibiting traits linked to human cognition, such as learning and problem solving, might be included under this umbrella term [41].

4.3 Applications of Artificial Intelligence

Artificial intelligence has a wide range of applications and can be applied to many different fields, including the following [42]:

4.3.1 Games

Artificial intelligence is used in computer programs that play chess in the world of gaming. These machines have to analyse every move very thoroughly since, in chess, winning is the ultimate objective, and every move affects that aim.

4.3.2 Self-driving cars

Autonomously operating vehicles do not require a driver to be present; they can function on their own. These vehicles' computer systems analyse outside data to generate collision-avoidance judgments. This technology is based on computer algorithms that can learn and adapt, which makes them able to accomplish jobs that were thought to be difficult in the past. Self-driving car deployment is progressively becoming more common in real-world traffic situations.

4.3.3 Search engines

A search engine is a technology that lets people look up information online or locally. Artificial intelligence, which is used on the web as robots, is necessary for it to function. These robots scan a variety of websites, index them, categorize the information, and decide which search phrases will appear first in the presentation order. One such system is the Google search engine.

4.3.4 Medical

Artificial intelligence is used in the medical industry for patient care, hospital procedures, clinical and basic research, and medical assessments. Artificial Intelligence is crucial in the process of drug dosage, therapy administration, operating room operations, and medical picture recognition and classification.

4.3.5 Industry

Industry 4.0 has benefited greatly from artificial intelligence, which uses clever algorithms to increase industrial process efficiency. Within the domain of condition-based maintenance, artificial intelligence (AI) keeps an eye on production procedures, minimizes malfunctions, lowers energy usage, and enables automated quality control to guarantee maximum output and better planning.

4.4 Machine Learning

As a subset of artificial intelligence, machine learning (ML) refers to a set of methods that provide computers the ability to learn and improve their performance on tasks, allowing them to handle issues without the need for explicit programming [43]. Machine learning, according to Arthur Samuel (1959), is the process of giving computers the ability to learn without the need for explicit, direct programming.

4.4.1 Machine Learning types

Based on their goals, machine learning types can be divided into four major groupings [44]:

4.4.1.1 Supervised Learning

Building a model that can forecast response values for a fresh dataset is the goal of supervised learning. The input data needs to be divided into features and labels prior to training. The algorithms classify new, uncategorized data and forecast outcomes using this categorized data. A testing dataset is frequently used in order to validate the model. You can use supervised learning to solve two kinds of problems:

- **Classification problem**

Discrete answer values are subjected to classification, which divides the data into several classes. Data classification using recognizable and classificable features is its aim [45].

- **Regression problem**

When dealing with continuous response values involving a continuous variable, regression is utilized. The model is trained to anticipate different variations and oscillations in real data through supervised learning [46].

4.4.1.2 Unsupervised Learning

In unsupervised learning, a dataset is given to an algorithm, which divides the heterogeneous collection of data into smaller groups. This method creates homogeneous clusters, which are collections of related data. The most common technique in unsupervised learning is "clustering," which involves identifying groups in the data through an exploratory study. Based on a similarity metric, which is frequently determined by metrics like probabilistic or Euclidean distance, clusters are created [47].

4.4.1.3 Semi-Supervised Learning

A hybrid method that incorporates aspects of both supervised and unsupervised learning is called semi-supervised machine learning. This approach works with a large amount of unlabeled data and a small amount of labeled data. Semi-supervised learning combines the best features of supervised and unsupervised learning, allowing for the use of unlabeled data with the direction of a lesser amount of labeled data. By using this method, training a model to label data can be accomplished with less reliance on large amounts of labeled training data.

4.4.1.4 Reinforcement Learning

Within the field of decision-making research, reinforcement learning (RL) teaches people how to respond optimally by seeing and interacting with their surroundings. Like a youngster investigating its environment and discovering the best ways to accomplish an objective, RL functions best in uncharted territory.

In order to find answers, artificial intelligence in this learning paradigm is faced with a trial-and-error situation. The program strives to optimize the total reward by earning incentives or penalties for its activities. Applications of reinforcement learning can be found in many fields, such as autonomous vehicles, game theory, and robot perception and movement.

4.5 Ensemble learning

Ensemble learning is a technique in machine learning that involves combining multiple models to achieve better performance than individual models alone. Here are its types, principles, and advantages:

4.5.1 Ensemble learning types:

- **Bagging (Bootstrap Aggregating):** Creates multiple subsets of the training data by random sampling with replacement and trains a model on each subset. The final prediction is made by averaging the predictions (for regression) or voting (for classification).
- **Boosting:** Sequentially trains models, each trying to correct the errors of its predecessor. Popular algorithms include :extremely randomized tree (ERT), AdaBoost, Gradient Boosting, and XGBoost.
- **Stacking:** Combines multiple models (base learners) and uses a meta-model to learn how to best combine their predictions.

4.5.2 Ensemble learning principle:

The core principle of ensemble learning is that a group of weak learners can come together to form a strong learner. By aggregating the outputs of various models, ensemble methods can reduce the risk of overfitting, minimize bias, and increase predictive performance [48].

4.5.3 Ensemble learning advantages:

- **Improved Accuracy:** By combining multiple models, ensemble methods often yield more accurate and reliable predictions.

- **Robustness:** Ensemble learning reduces the impact of noisy data and mitigates the weaknesses of individual models.
- **Versatility:** Applicable to various types of machine learning problems, including classification, regression, and anomaly detection.
- **Reduction of Overfitting:** Techniques like bagging and boosting help in decreasing the variance and bias of the model, leading to better generalization on new data.

Ensemble learning has become a fundamental strategy in machine learning competitions and real-world applications, offering significant performance enhancements over single models.

4.6 Features classification algorithms

4.6.1 K-Nearest Neighbors (KNN)

A simple non-parametric method for supervised classification that doesn't require model development is the K-Nearest Neighbors (KNN) algorithm. It uses integer data to function [49]. The number of predictor variables, n, is represented for each observation in the training dataset by this approach in an n-dimensional space.

In order to forecast which class a new observation belongs to, the method uses the training data to compute the Euclidean distance, which allows it to find the k closest instances to the new observation. It then chooses the majority class from its k closest neighbors to designate the anticipated class.

4.6.2 Decision Tree (DT)

Recursive partitioning is employed by the decision tree approach, which can be used for both regression and classification. It makes use of a tree model, in which every level denotes a class and every node represents a test on a single feature. Conditions applied to one of the features determine the decisions. These conditions are represented by internal nodes, while the final choice based on the applied conditions is embodied by leaf nodes [50].

4.6.3 Random Forest (RF)

The random forest algorithm was first presented by Leo Breiman and included a random element. By adding randomization to the selection of variables used in the models, this innovation seeks to improve the independence of aggregated trees [51].

The random forest is made up of several decision trees working together. Every single tree in the random forest makes a class prediction, and all of the findings that each tree produces together provide a collective vote that determines the final prediction model.

As one of the most successful ensemble learning techniques, the random forest (RF) uses a large number (hundreds to thousands) of separate decision trees to perform well on classification and regression problems. As an ensemble approach, RF combines the ideas of bagging and random feature selection by using several decision trees as weak classifiers or regressors. The RF is a representative ensemble classifier that is built using a variety of decision trees. It has gained popularity because of its exceptional classification accuracy and operational efficiency, which have led to its widespread use in a variety of fields.

4.6.4 Extremely Randomized Trees (ERT)

As an extension of the Random Forest (RF) algorithm with a focus on maximizing randomization, the Extremely Randomized Trees (ERT) approach was first presented by Geurts et al..[52]. It is a member of the randomized tree family. Like RF, ERT has strong training capabilities and is computationally efficient, especially for high-dimensional input vectors. Significantly, ERT performs faster than RF in terms of training speed, which is explained by ERT's easier method for choosing thresholds. Moreover, ERT has reduced variation due to its increased randomization. The fact that ERT trees are separately trained utilizing the complete set of training data points is another unique characteristic.

Although both RF and ERT are part of the ensemble learning models that use the decision tree algorithm, their fundamental approaches are different. Random Forest (RF) uses replacement sampling to subsample the data in order to produce randomness. This procedure adds value to the dataset and helps create a model with very unique training data.

ERT, on the other hand, uses the complete dataset, which lowers bias and improves the performance of the model. Moreover, they take different ways to splitting nodes: ERT splits nodes at random, while RF looks for the best split. In highly randomized trees, the random split contributes to the reduction of data variance. The goal of both ERT and RF is to strike the ideal ratio between bias and variance. They are chosen using the ensemble of decision trees, which performs better than the conventional decision tree technique.

Although an ERT classifier and an RF are similar, they differ in that randomization is included during the training process. An ERT classifier trains several trees, each of which is trained using the complete dataset. Analysing a portion of all available features is what the optimal node-level split entails, much like the random decision forest. Rather than trying to find the ideal threshold for every feature, a single, randomly selected threshold is used for every feature. Based on these random divisions, the division that results in the largest rise in the employed scale score is then chosen. More independent trees are produced as a result of the increased randomization during training, which further lowers variance. As a result, highly randomized trees typically produce better outcomes than random forests.

4.6.5 Support Vector Machines (SVM)

Vapnik et al. introduced Support Vector Machines (SVM) [53], a kind of machine learning approach with roots in statistical learning theory that tackles function approximation problems. Statistical interference resulting from a finite number of observations is addressed by this method, especially in supervised binary classification. Support Vector Machines (SVM) were first presented by Vapnik as a technique for region separation. Finding the ideal hyperplane to divide data points into two different groups is the main goal of support vector machines

The concept of this method is to define a decision function: $S: X \rightarrow \{-1,\ 1\}$ with a simple set of data$\{(x_{i,}\ y_i);\ x_i \in X\ and\ y_i\ \in\ (-1, 1)\}$. A decision function for each new point x∈ X, predicts its membership in the correct class ((-1) or (+1)). This was done by minimizing the structural risk, which is able to approximate by the empirical model. [47].

- **Case of linear classification**

In case of linear classification, SVM algorithm purpose is to find a hyperplan that separate at best the samples of two classes. Assume that the following empirical data

$(x_1, y_1) \dots (x_i, y_i) \dots (x_m, y_m) \in R \times \{\pm 1\}$ are considered, the function S is linear in x_i with the following general form: $(x_i =< w, x_i >) + b$. (5.1)

Figure 1 shows that the provided data can be separated by a large number of hyperplanes. The ideal solution among these is represented by just one hyperplane. The following requirement is taken into consideration in order to identify the ideal hyperplane:

$$y_i(wx_i + b) \geq 1 \; for \; i = 1 \; \dots m \qquad (5.2)$$

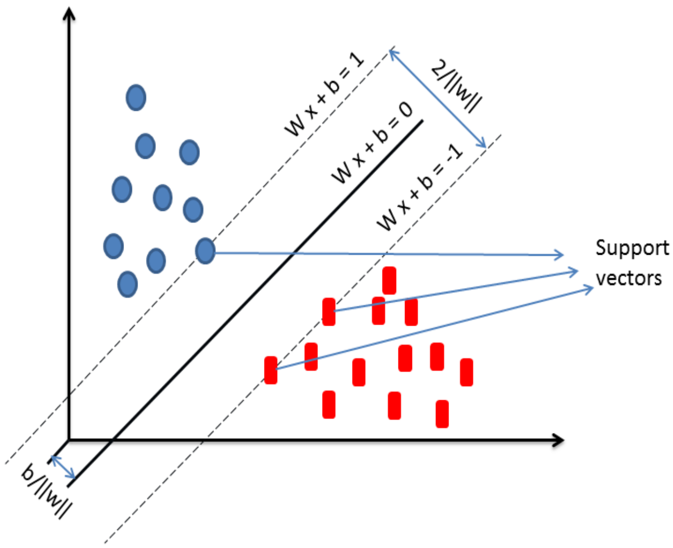

Figure 4.1: SVM hyperplane in linear representation.

The optimization task can be expressed as below:

$min_{x \in X} f(x)$ under the constraint $g_i(x) \leq 0$. The Lagrangian method can be used to solve this kind of problems which could be expressed as:

$$\begin{cases} \sum_i^L \propto_i - \frac{1}{2} \sum_{i,j}^L \propto_i \propto_j y_i y_j < x_i, x_j > \\ \propto_i \geq 0 \\ \sum_i^L \propto_i y_i = 0 \end{cases} \qquad (4.3)$$

Where $\propto_i$ represents the Lagrangian parameters.

$\propto_i \neq 0$ for $y_i(< w, x_i > +b) = 1$

$\propto_i = 0$ for $y_i(< w, x_i > +b) > 1$

The obtained weight hyperplan vector $w = \sum_{i=1}^{L} \propto_i y_i x_i$ and the offset $= 1 - < w, x_i >$, where x_i is support vector of the know class. Finally, the hyperplan function is defined as:

$$f(x) = < w, x > +b \ = \sum_{i \in SV} \propto_i y_i < x_i, x > +b \qquad (5.4)$$

- **Case of nonlinear classification**

The hyperplane separator covered in the preceding section loses its usefulness in nonlinear classification. This means that a nonlinear Support Vector Machine (SVM) must be used. The main idea is to find the maximum dimension space, represented by a Hilbert space H based on a scalar product, in which the examples' projections are linearly separable. This is illustrated in Figure 2. An observation space kernel function can take the place of this scalar product.

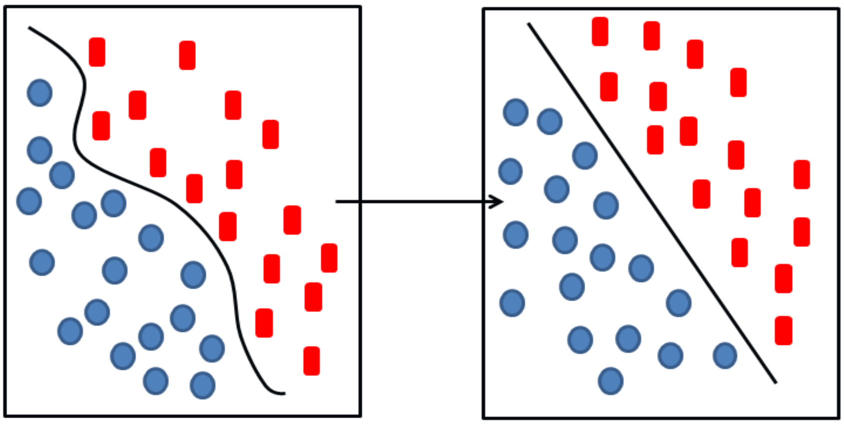

Figure 4.2 : SVM hyperplane in nonlinear representation.

We suppose:

$$\emptyset : R^P \rightarrow H ; x_i \mapsto \emptyset(x_i) \qquad (4.5)$$

The substitution the scalar product $< \emptyset(x_i), \emptyset(x_j) >$ by a kernel function $K(x_i, x_j)$, permits the problem of optimization to be defined as :

$$\begin{cases} max_{\propto_i} \sum_i^L \propto_i - \frac{1}{2} \sum_{i,j}^L \propto_i \propto_j y_i y_j K(x_i, x_j) \\ \sum_i^L \propto_i y_i = 0 \\ C \geq \propto_i \geq 0 \end{cases} \tag{4.6}$$

(10)

C denotes the tolerance constant. Finally, the decision function defined as:

$$f(x) = < w, x > +b = \sum_{i \in SV} \propto_i y_i K < x_i, x > +b \tag{4.7}$$

Applications for Support Vector Machine (SVM) may be found in many domains, but in industrial equipment, SVM is very useful for identifying and diagnosing electromechanical systems problems.

4.7 Classification evaluation and Metrics

Classification is a fundamental task in machine learning and data science, involving the assignment of categorical labels to instances based on their features. Evaluating the performance of classification models is crucial to ensure their reliability and effectiveness in real-world applications. Classification evaluation metrics provide quantitative measures to assess how well a model is performing and to compare different models.

4.7.1 Polygon Area Metric

Because of its stability and thorough measurement, the Polygon Area Metric [54], is used to assess the performance of a single-scale classifier.

A polygon is constructed using six established metrics (CA, SE, SP, AUC, JI, and FM), from which the equivalent area for PAM is computed. Here are the theoretical calculations:

$$\text{Classification Accuracy} = CA = \frac{TP+TN}{TP+TN+FP+FN} \tag{4.8}$$

$$\text{Sensitivity} = SE = \frac{TP}{TP+FN} \tag{4.9}$$

$$\text{Specificity} \quad = \quad SP \ = \ \frac{TN}{TN+FP} \tag{4.10}$$

$$\text{Jaccard Index} \quad = \quad JI \ = \ \frac{TN}{TN+FP} \tag{4.11}$$

$$\text{F-measure} \quad = \quad F \ = \ \frac{2TP}{2TP+\ FP+FN} \tag{4.12}$$

$$\text{Area Under Curve} \quad = \quad AUC = \int_0^1 f(x)\,dx \tag{4.13}$$

Where the numbers TP, TN, FP, and FN stand for the number of positive and negative samples that were correctly predicted and the number of positive and negative samples that were wrongly forecasted, respectively. The receiver operating characteristic curve, f(x), is created by plotting the true-positive rate (SE) against the false-positive rate (1-SP) at various cut-off points R. It is significant to remember that SE and SP relate to the proportions of class 1 and class 2 samples in the overall population that were correctly identified.

The PAM computation uses the area of the polygon formed by the CA, SE, SP, AUC, JI, and FM points in a regular hexagon, as shown in Figure (5.3). It is interesting to observe that the regular hexagon is made up of six equilateral triangles, with a side length of one. It is therefore correct to say that the area of 2.59807 is equal to |OP1| = |OP2| = |OP3| = |OP4| = |OP5| = |OP6| = 1.

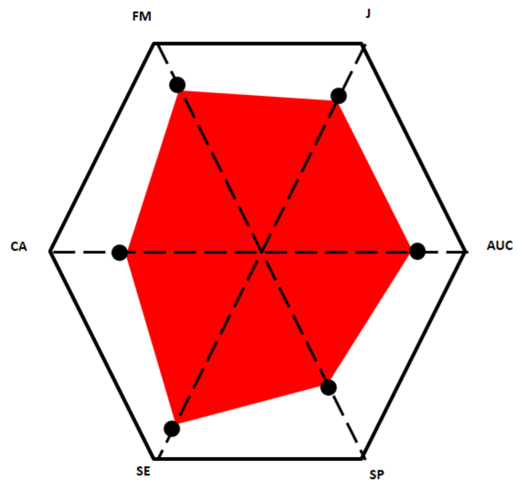

Figure (4.3): Polygon in regular hexagon.

The values of CA, SE, SP, AUC, JI, and FM are corresponding to the lengths |OP1|, |OP2|, |OP3|, |OP4|, |OP5|, and |OP6|, respectively. The following formula is used to calculate the PAM:

$$PAM = \frac{PA}{2.59807} \tag{4.14}$$

The area of the polygon is PA.

It should be noted that dividing the PA value by 2.59807 guarantees the normalization of the PAM into the [0, 1] interval.

4.8 Conclusion

Overview of artificial intelligence has been presented in this chapter, with a particular emphasis on machine learning and its different applications, especially in the context of categorization problems. Furthermore, various assessment instruments and metrics have been investigated to ascertain the efficacy of categorization models. The contribution of innovative defect detection techniques in transformers and induction motors will be covered in detail in the following chapter.

Chapter 5: Contribution to the faults diagnosis of electrical systems

5.1 Introduction

Maintaining the overall reliability of electrical equipment and cutting maintenance costs need close attention to machine condition. This is especially important for electrical transformers and induction motors, which are essential parts of electromechanical systems used for distribution and transmission. These parts' failures may cause serious harm, power outages, and expensive repair bills. This chapter introduces a novel non-contact, non-intrusive experimental paradigm for defect diagnosis and monitoring in electrical transformers and induction motors. The methodology combines machine learning techniques with infrared thermography (IRT).

The suggested method works step-by-step, starting with the use of infrared thermography (IRT) to take thermographic pictures of the intended machine. Afterwards, features relating to faults are extracted from the IRT images using feature extraction algorithms. Lastly, different defect patterns are automatically identified by applying machine learning classifiers.

Experimental IRT images are used to assess the effectiveness of the suggested method, and the diagnostic results demonstrate its strong performance. It is shown to be a powerful diagnostic instrument with significant classification accuracy and stability above previously used techniques.

5.2 1st Contribution: Induction motor faults diagnosis

5.2.1 Data base

A three-phase, 1.11 kW, 5 A, 220/230 V induction motor was used for the experiments. In order to identify eight distinct short-circuit defects in the stator windings as well as an induction motor that was working normally, thermal images were methodically taken and examined. It is imperative to stress that every anomaly found in this dataset was caused by internal flaws, unrelated to external components or electrical component problems during initial setup [55].

A Dali-tech T4/T8 infrared thermal imaging camera was used to capture the thermal images on a workbench in the Electrical Machines Laboratory, with the room temperature being 23°C. Table 5.1 lists the particular attributes of the thermal camera and the induction motor's specifications.

Table 5.1: lists the characteristics of the induction motor and the thermal camera [55].

properties of the used thermal camera	
Dali-tech T8 TIC	
Detector resolution	384*288
Measurement accuracy	±2° or ±2% (of reading, which is greater)
Imaging NETD	⩽ 0.04°@30°
Measuring range	-20°- +650°
Imaging Frame Rate	50/60Hz
Induction motor specifications	
Phase	Y-3
Power	1.11-KW
Voltage	220/380V
Input Current	5A
Speed	2800RPM
Frequency	50Hz

The induction machine is shown in nine image sets in a variety of states, including eight distinct malfunctioning circumstances and a healthy state. "α-phase" denotes the number of phases impacted by short-circuit flaws, whereas "%-stator" represents the short-circuit rate for each phase. Table 5.2 provides an overview of the specifics of these states.

Table 5.2: provides an overview of the nine states taken into account in the induction motor faults diagnosis [55].

Stator Fault class	0 %	50%		30%			10%		
α-phase	Healthy	A&B	A	A&B&C	A&C	A	A&B&C	A&C	A
Class label	1	2	3	4	5	6	7	8	9

Figure 5.1 shows the thermal pictures taken under both ideal and faulty settings. It is clear that it is difficult to look for and discover flaws by looking at thermographs directly. It is challenging to identify distinct variations between thermal pictures taken under normal and unhealthy conditions, which could result in inaccurate and misleading classifications. This highlights the need for further study and the application of cutting-edge techniques in artificial intelligence and machine learning to enhance the ability to distinguish between the situations that are being looked into.

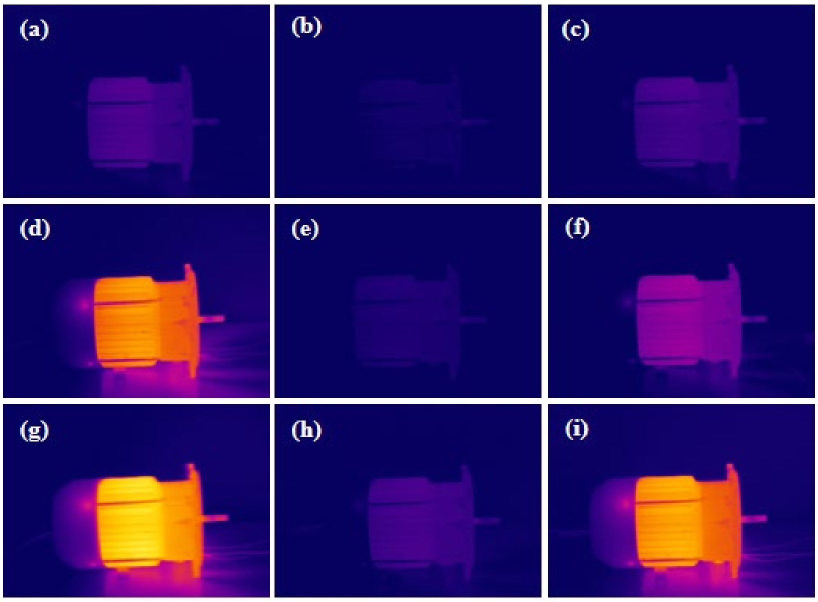

Figure 5.1: thermal image of induction motor: (a) Healthy, (b) 10% in phase A, (c) 10% in phase A&C, (d) 10% in phase A&B&C, (e) 30 % in phase A, (f) 30 % in phase A&C, (g) 30 % in phase A&B&C, (h) 50 % in phase A, (i) 50 % in phase A&C [55].

5.2.2 Proposed Method

Within the framework of this thesis, a new approach to the faults diagnosis of induction motors is presented. As shown in the flowchart in Figure 5.2, this strategy uses SURF-BoVW (Speeded-Up Robust Features - Bag of Visual Words) for feature extraction in conjunction with an Extremely Randomized Trees (ERT) Classifier. The first stage is to use the SURF method to extract a set of features (visual words) from the Infrared Image Thermography (IRT) data. After that, k-means clustering is used to encode the extracted characteristics, resulting in the creation of a histogram. After then, the feature set is split into training and testing samples at random.

Finally, classification is done using the ERT classifier. The testing samples are classified using the predetermined parameters following the conclusion of the training phase and the establishment of the ERT classifier parameters.

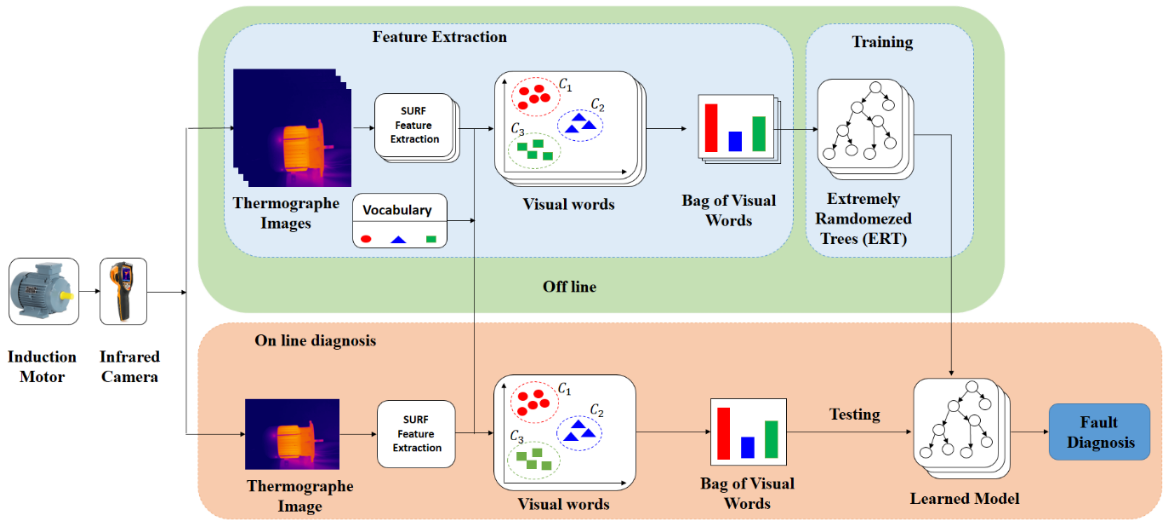

Figure 5.2: Overview of the proposed method.

5.2.3 Obtained results and discussion

We perform a comparison analysis with several classification approaches, such as KNN, DT, SVM, Least Squares Support Vector Machine (LSSVM), Self-organizing Fuzzy Logic Classifier (SOF), Random Forest (RF), and Deep Rule Based (DRB), to demonstrate the robustness of the suggested method. We also use standard deviation over 10 experiments to evaluate the stability of the classification approach, taking into account average, maximum, and minimum values to account for any contingencies.

The feature set that was retrieved by BOVW and SURF is used as input for each classification method, which includes SVM, Decision Trees (DT), KNN, Least Squares Support Vector Machine (LSSVM), Random Forest (RF), and Deep Rule Based (DRB). Important details for every approach are listed: SVM employs a kernel function of 0.01 with a penalty factor of 100; DT sets a minimum of five father nodes; KNN views K = 5 as the nearest neighbor number; and LSSVM uses a regularization value of 10,000 along with a Gaussian kernel function of 0.5.

Table 6.3 provides specifics on the categorization outcomes for every technique. Notably, as compared to other techniques, KNN shows reduced classification accuracy. Furthermore, the standard deviation emphasizes the instability of KNN's classification method by highlighting the inconsistent categorization influence of the network on different testing samples.

Compared to SVM, KNN has a higher standard deviation and a poorer average classification accuracy, with differences of 0.0015 and 3.7700%, respectively. The classification accuracy of SVM has a standard deviation of 0.0308. SVM exhibits a 10.2% higher minimum classification accuracy than ERT, despite its algorithmic instability.

For SOF, DT, SVM, LSSVM, RF, and DRB, the highest possible classification accuracy is 100%. They do, however, have a larger classification accuracy standard deviation than the ERT classifier. An important factor affecting the classification accuracy of SOF, DT, LSSVM, RF, and DRB is the input of distinct samples.

Table 5.3: displays the classification outcomes of the tested techniques, which include decision trees (DT), ERT (extremely randomized trees), KNN (k-nearest neighbor), SOF (self-

organizing fuzzy logic classifier), RF (random forest), DT (decision tree), SVM (support vector machine), and LSSVM (least squares support vector machine).

	KNN	SOF	ERT	DT	SVM	LSSVM	RF	DRB
MAX	0,9815	1,0000	1,0000	1,0000	1,0000	1,0000	1,0000	1,0000
MIN	0,8796	0,9444	1,0000	0,9259	0,8981	0,9630	0,9815	0,9537
MEAN	0,9466	0,9779	1,0000	0,9786	0,9843	0,9879	0,9972	0,9815
STD	0,0293	0,0171	0,0000	0,0260	0,0308	0,0138	0,0070	0,0169

RF has a significantly greater average categorization accuracy than ERT. The suggested method's classification stability is more resilient than RF's, based on the standard deviation of classification accuracy.

All things considered, our method produces higher and more dependable classification results because it attains the best overall classification accuracy out of all the examined methods. Figures. 5.3 and 5.4 show the confusion matrix and the classification results of the previously stated approaches in the eighth experiment, respectively, to provide an intuitive depiction of the classification impacts from various methods.

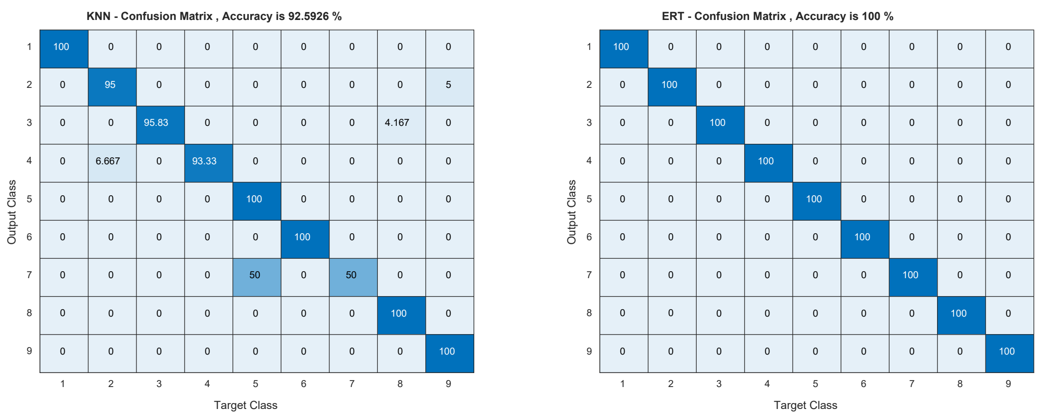

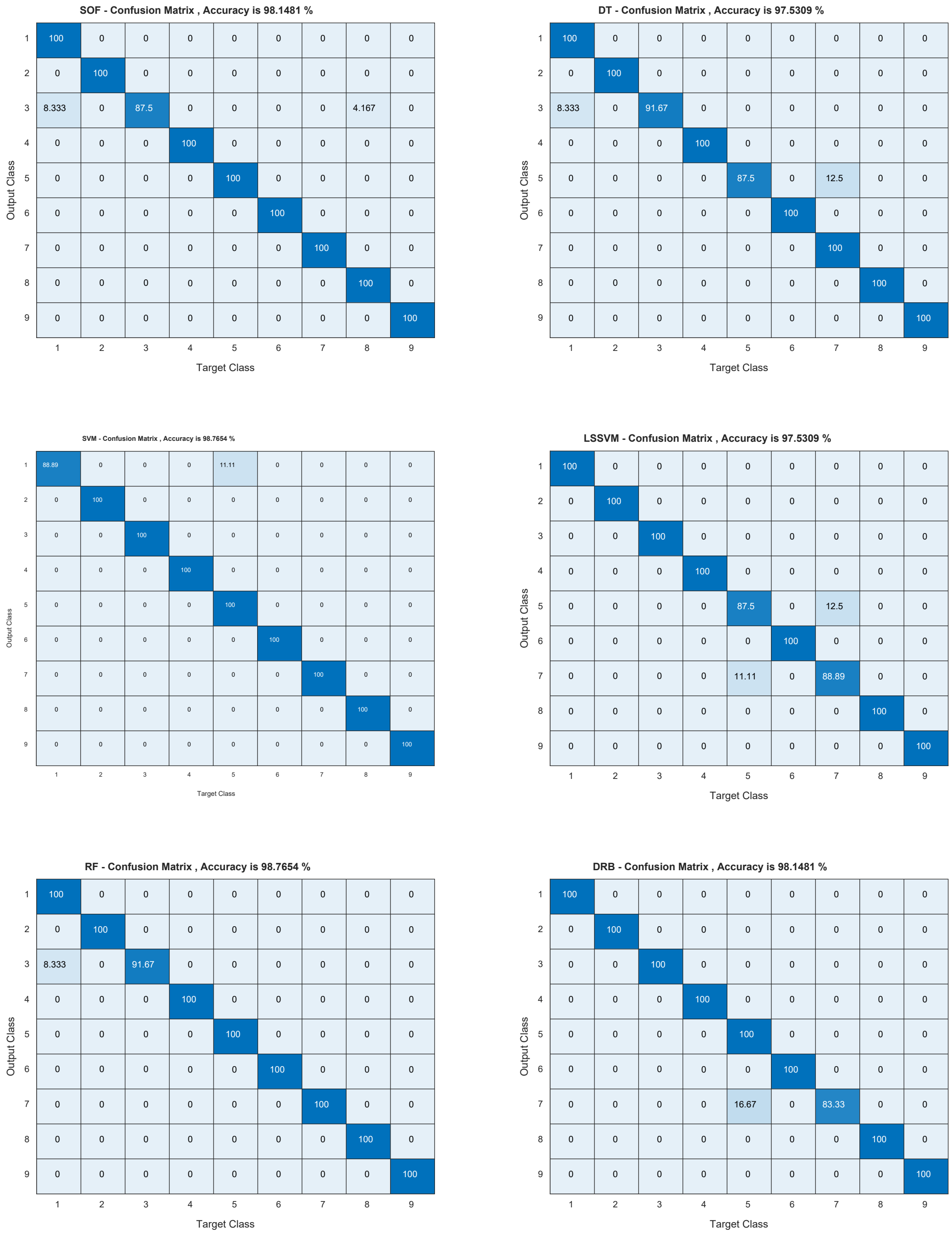

Figure 5.3: Confusion matrix of each classification method in the 8th experiment. (KNN, ERT, SOF, DT, SVM, LSSVM, RF and DRB).

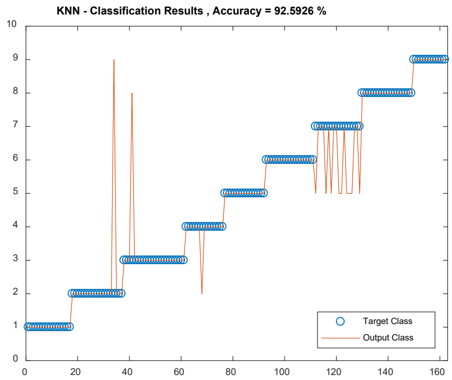
KNN - Classification Results , Accuracy = 92.5926 %
Target Class
Output Class

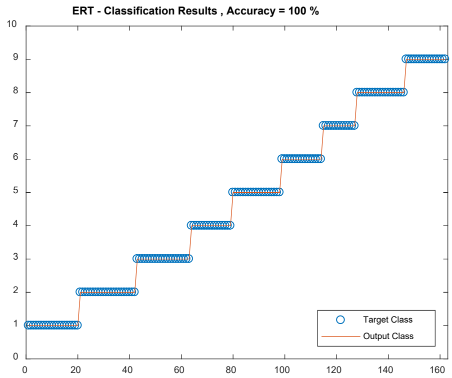
ERT - Classification Results , Accuracy = 100 %
Target Class
Output Class

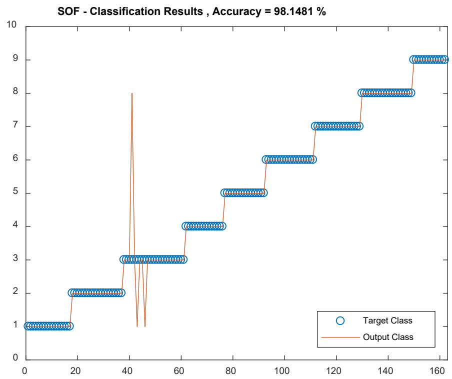
SOF - Classification Results , Accuracy = 98.1481 %
Target Class
Output Class

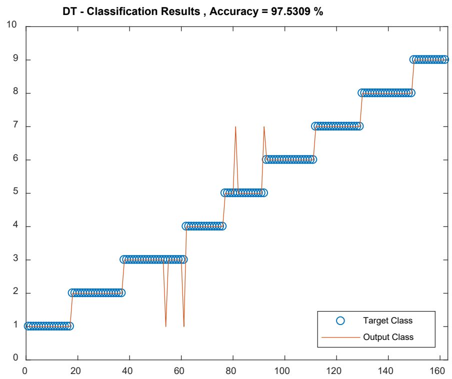
DT - Classification Results , Accuracy = 97.5309 %
Target Class
Output Class

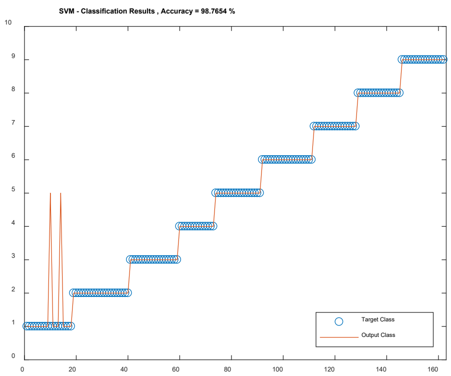
SVM - Classification Results , Accuracy = 98.7654 %
Target Class
Output Class

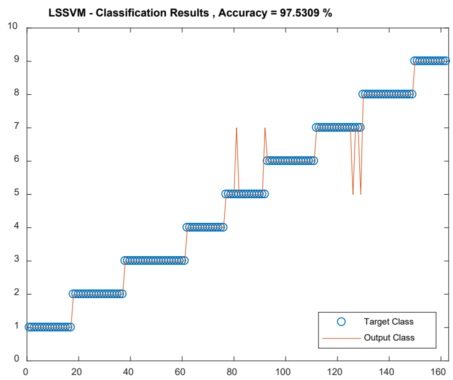
LSSVM - Classification Results , Accuracy = 97.5309 %
Target Class
Output Class

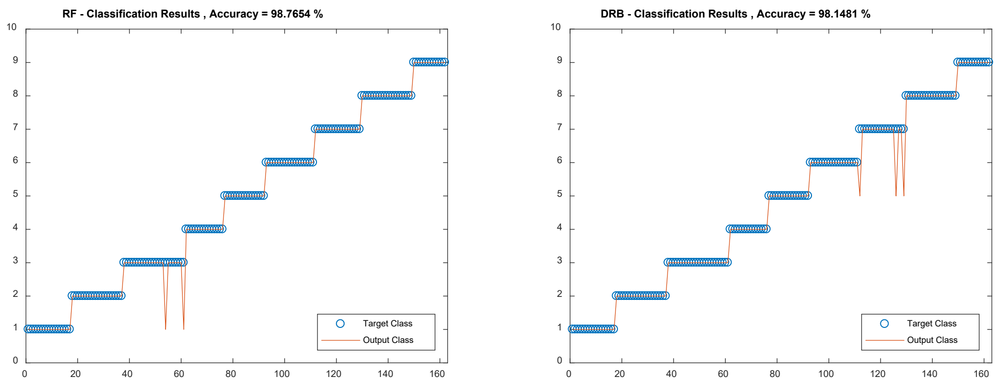

Figure 5.4: The eighth experiment's classification outcomes for each classification technique. (Classification results for KNN, ERT, SOF, DT, SVM, LSSVM, RF, and DRB).

With a classification accuracy of 92.5926%, KNN appears to have the lowest performance in the confusion matrix figure. There are significant errors in categories 2, 3, 4, and 7. In particular, roughly 4% and 6% of test samples are misclassified for categories 3 and 4, while 50% of samples are misclassified for category 7. About 5% of test samples are misclassified for category 2.

Of the testing samples, 7.4074% are misclassified according to the KNN classification results. For example, category 2 makes up 5% of the total, category 7 makes up 50% of the total, category 3 makes up 4.163% of the total, category 8, and category 4 makes up 6.667% of the total.

Both SOF and DRB show a total misclassification rate of 1.8519% in the classification results. On the other hand, 8.33% of category 3 samples are wrongly allocated to category 1 and 4.167% of category 3 samples are assigned to category 8 by the SOF classifier. 16.67% of category 7 samples in the DRB are incorrectly categorized as category 5.

Comparably, the classification results of DT and LSSVM show a total misclassification rate of 2.4691%. In particular, 12.5% of category 5 samples are incorrectly categorized as category 7, and 8.333% of category 3 samples are incorrectly labeled as category 1 in the DT classifier. However, in the instance of LSSVM, 11.11% of category 7 samples and 12.5% of category 5 samples are incorrectly classified as category 7.

In their classification results, the SVM and RF classifiers show a cumulative misclassification rate of 1.2346%. Interestingly, 11.11% of category 1 samples were incorrectly classified as category 7 by the SVM classifier. On the other hand, 8.33% of category 3 samples were incorrectly classified as category 1 by the RF classifier.

There are no examples of samples that were incorrectly classified in the classification results of the suggested approach (ERT), and the classification accuracy is 100%.

Moreover, a comprehensive analysis of the experimental results from various angles is carried out with the Polygon Area Metric (PAM). The findings of the Polygon Area Metric for each classification technique used in the eighth experiment are shown graphically in Figure 5.5.

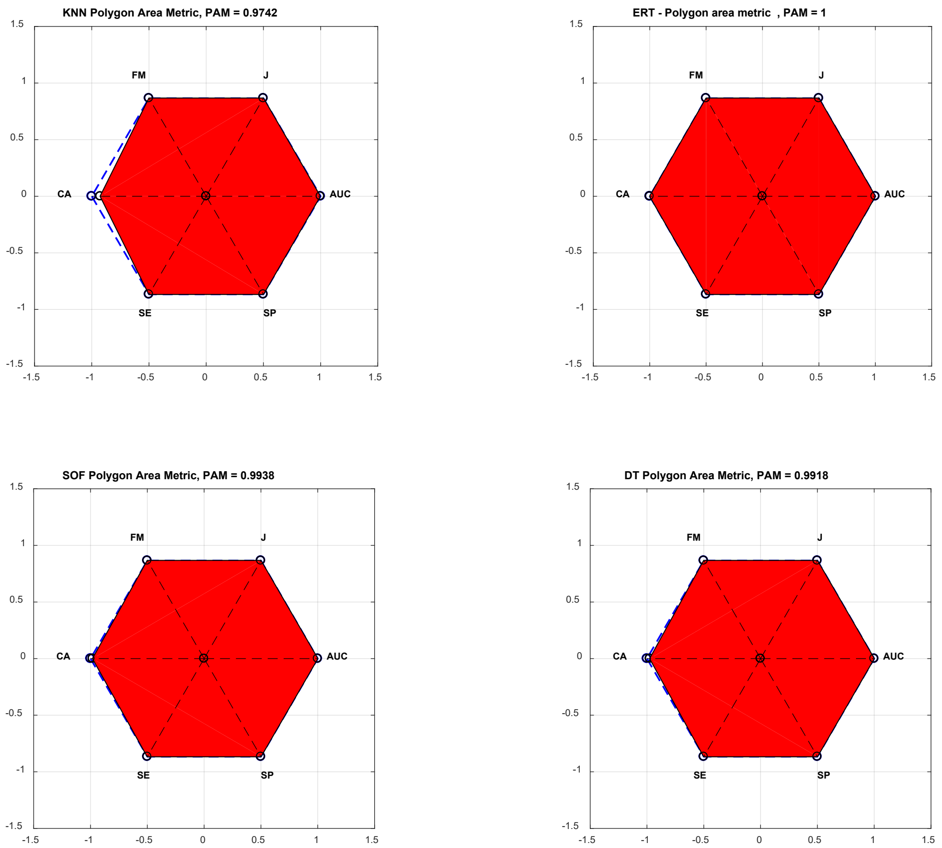

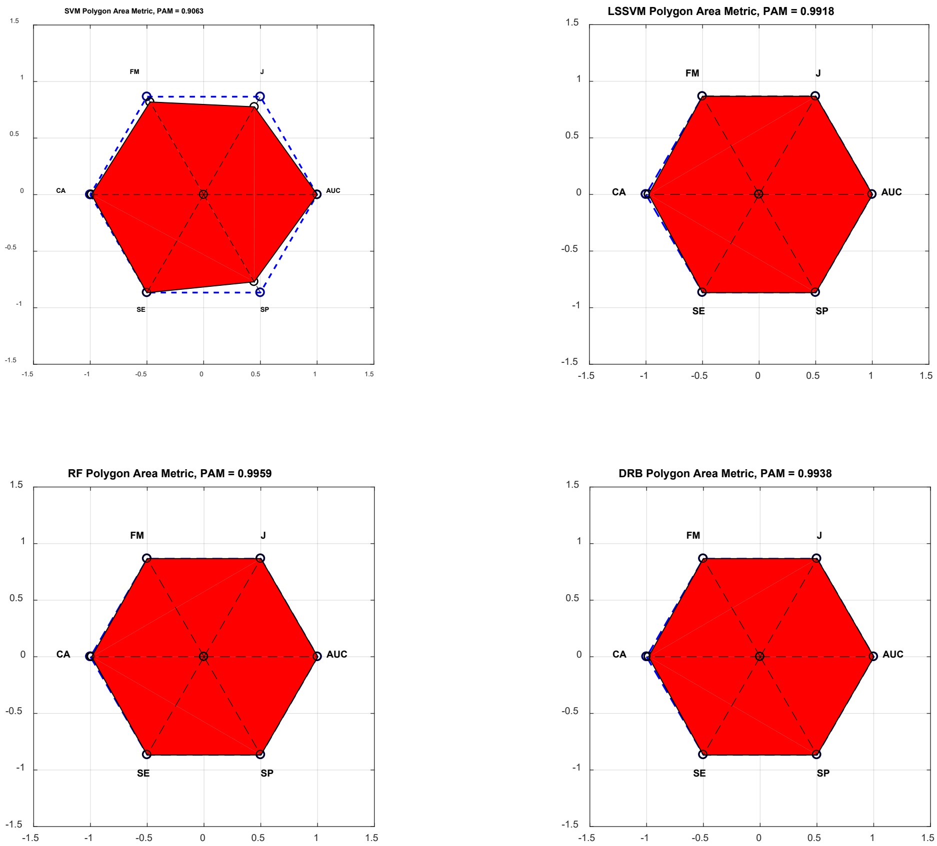

Figure 5.5: Area metric graphs in polygons for every classification technique used in the eighth experiment. (KNN, ERT, SOF, DT, SVM, LSSVM, RF, DRB).

The extent to which the PAM for each classification method is covered may be seen from these graphical representations; ERT shows the most advantageous Polygon Area Metric, followed by the other classifiers.

5.3 2nd Contribution: Transformer faults diagnosis

5.3.1 Data base

The thermal imaging data was captured for training and testing in the electrical transformer investigations. This dataset included eight different instances of short circuit failures in the common core winding in addition to a healthy state. It is imperative to stress that every defect found in this dataset is an internal issue, unrelated to external components or malfunctions in the electrical components' initial configuration [56].

At 23°C ambient temperature, thermal image acquisition was carried out on a workbench in the Electrical Machines Laboratory using a Dali-tech T4/T8 infrared thermal imaging camera. Table 5.4 lists the exact characteristics of the electrical transformer and the thermal camera.

Table 5.4: Thermal camera properties and electrical transformer specifications [56].

Thermal camera properties	Transformer specifications
Dali-tech T8 TIC Detector resolution 384*288 Measurement accuracy ±2° or ±2% (of reading, which is greater) Imaging NETD ⩽ 0.04°@30° Measuring range -20°- +650° Imaging Frame Rate 50/60Hz	Phase 1 Power 1 KW Voltage 220 V Input Current 1.5 A Operating Voltage 220-660 Frequency 50-60 Hz

Nine sets of pictures show the electrical transformers in good condition and eight different defective states. Table 5 presents the number of short-circuit occurrences in the first column out of the 600 rounds, and the fault class percentage (%) that corresponds to the number of short-circuit occurrences is shown in the second line.

Table 5.5: General description of the nine considered states in the electrical transformers faults diagnosis [56].

Fault class (rounds)	Healthy	80	160	240	320	400	480	560	600
Fault class	0 %	13 %	26 %	40 %	53 %	66 %	80 %	93 %	100 %
Class label	1	2	3	4	5	6	7	8	9

Figure 5.6 displays the thermal pictures of both the healthy and defective states. It is difficult to see and detect flaws only by looking at thermographs directly because there are little variations between thermal images taken in healthy and unhealthy circumstances. Because of the unreliability of this visual classification, more research and the creation of novel methodologies based on machine learning and artificial intelligence will be required to better distinguish between the cases under study.

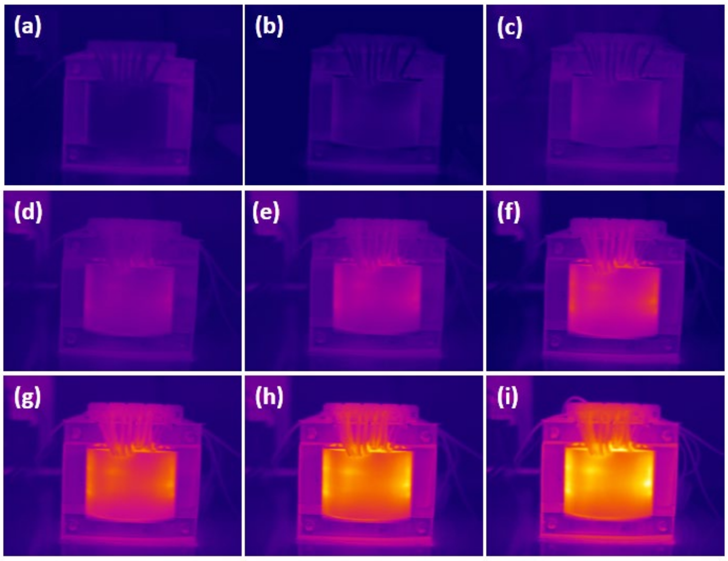

Figure 5.6: Heat-thermal image of electrical transformer: (a) healthy, (b) 13% fault, (c) 26% fault, (d) 40% fault, (e) 53% fault, (f) 66% fault, (g) 80% fault, (h) 93% fault, (i) 100% fault [56].

5.3.2 Proposed Method

A new method of using a Support Vector Machine (SVM) Classifier in conjunction with GIST feature extraction is provided for transformer condition monitoring. Figure 6.7 shows the flowchart for the suggested procedure. The first step after obtaining Infrared Image Thermography (IRT) is to use the GIST algorithm to extract a feature set. The SVM classifier is then applied for classification. Testing samples are categorized using the predetermined parameters after the SVM classifier's training phase and parameter fixation.

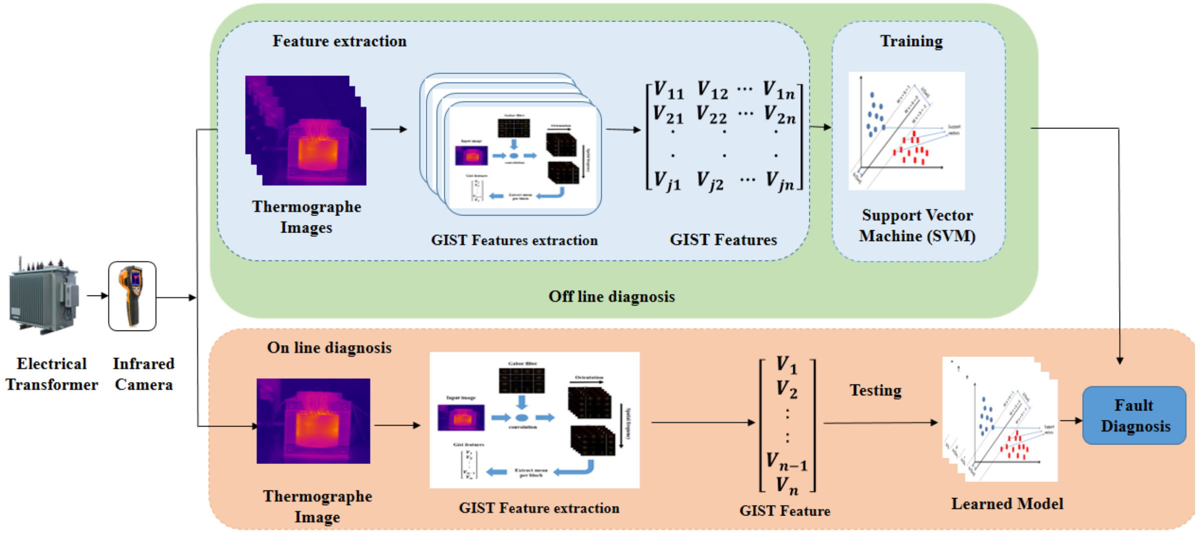

Figure 5.7: Global overview of the proposed method.

5.3.3 Obtained results and discussion

A comparative analysis with various classification techniques, such as K-Nearest Neighbor (KNN), Self-Organizing Fuzzy Logic Classifier (SOF), Extremely Randomized Tree (ERT), Decision Tree (DT), Extreme Learning Machine (ELM), Random Forest (RF), and Semi-Supervised Deep Rule-Based (SSDRB), is conducted in order to evaluate the robustness of the proposed method. Furthermore, the standard deviation across ten tests is used to assess the classification stability of the method, accounting for average, maximum, and minimum values to lessen the effect of contingencies.

The GIST-extracted feature set is used as input by all of the aforementioned classification techniques. The kernel function of the conventional Support Vector Machine (SVM) is 0.01 and the penalty factor is 100. The minimal number of father nodes for Decision Trees (DT) is five. The nearest neighbor number in KNN is K = 5. Table 6 displays the outcomes of every classification technique.

Table 6.6 illustrates how ELM's classification accuracy is comparatively lower than that of other approaches. Furthermore, the standard deviation illustrates the unstable nature of this method's classification algorithm by demonstrating the uneven effects it has on various testing samples. In terms of average classification accuracy and standard deviation, DT performs the worst after the ELM classifier, with differences of 0.896 and 0.039, respectively. The classifiers that come next are SOF, KNN, RF, and DRB. Their standard deviations vary from 0.032 to 0.015, and their average classifications lie between 0.956 and 0.967.

Table 5.6: Obtained Classification results, times and evaluations of the tested methods.

Classifiers / Evaluation metric		KNN	SOF	ERT	DT	ELM	RF	DRB	SVM
Time (s)		4.060	5.464	29.431	6.943	5.451	80.688	4.633	8.924
Classification _Accuracy (CA)	MAX	0,996	0,987	1	0,955	0,682	0,987	0,987	1
	MIN	0,882	0,873	0,980	0,828	0,377	0,923	0,936	0,980
	MEAN	0,960	0,956	0,995	0,896	0,532	0,956	0,967	0,995
	STD	0,032	0,028	0,007	0,039	0,077	0,021	0,015	0,005
Polygon Area Metric (PAM)	MAX	0,998	0,995	1	0,968	0,384	0,995	0,995	1
	MIN	0,933	0,957	0,993	0,704	0,072	0,898	0,939	0,993
	MEAN	0,979	0,985	0,998	0,846	0,177	0,963	0,986	0,998
	STD	0,019	0,009	0,002	0,077	0,091	0,026	0,013	0,001

Where, KNN: k-nearest neighbor, SOF: Self-organizing fuzzy logic classifier, ERT: Extremely randomized trees, DT: decision tree, ELM: Extreme Learning Machine, RF: random forest, DRB: Deep Rule Based and SVM: support vector machine.

Compared to SVM, the maximum, minimum and average classification accuracy of ERT is the same as the SVM, but if one focuses on the standard deviation of classification accuracy, the STD of the SVM is 0.05 better than ERT with equal to 0.07. That means that the classification stability of ERT is not as good as the proposed method.

Globally, the classification accuracy of the adopted method is the highest of all the tested methods. Consequently, its classification result is the best and the most reliable.

In order to offer an intuitive illustration of the classification effects resulting from various methods, Figures 6.8 and 6.9 respectively shows the confusion matrix and classification results of the previously discussed methods in the 6th experiment.

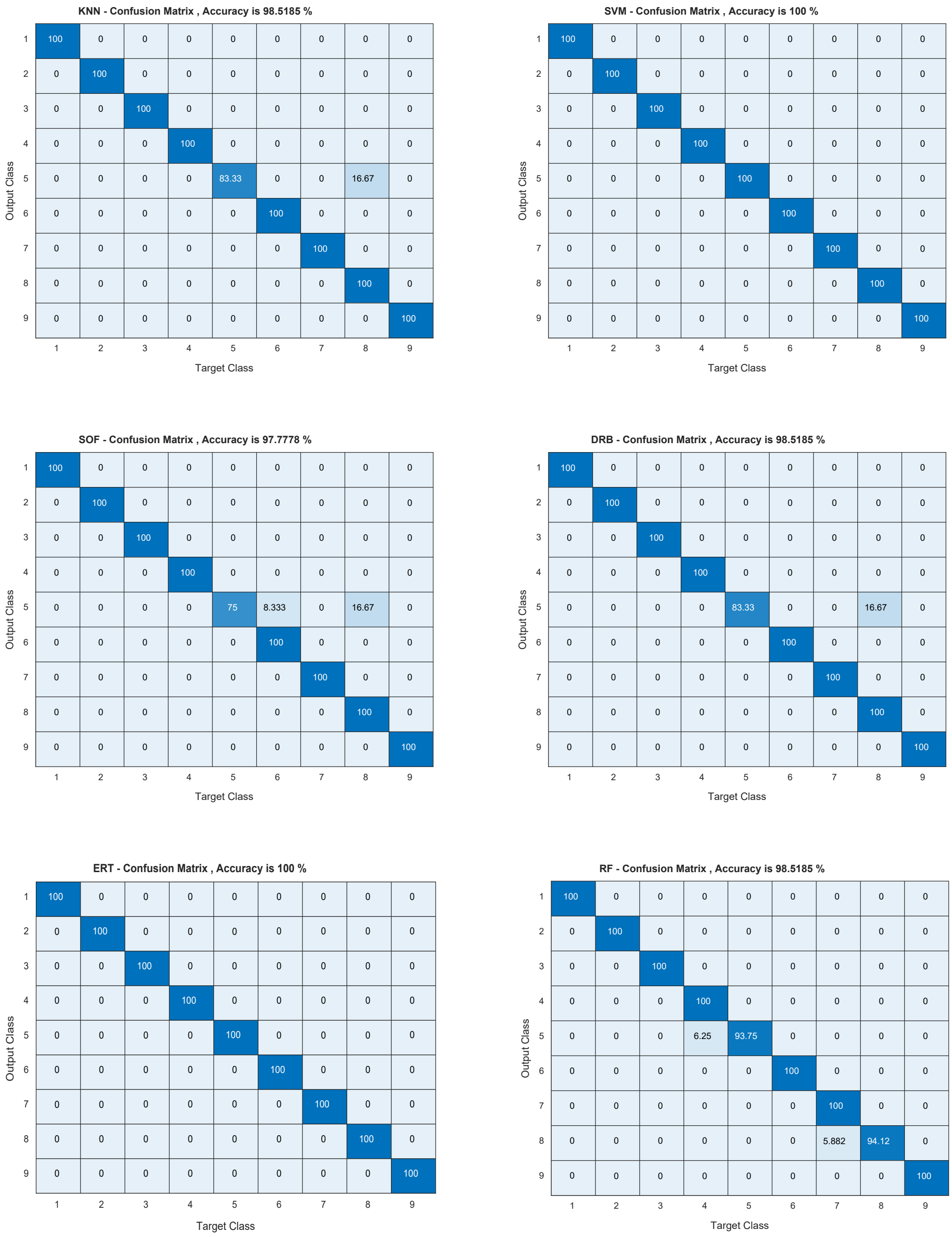

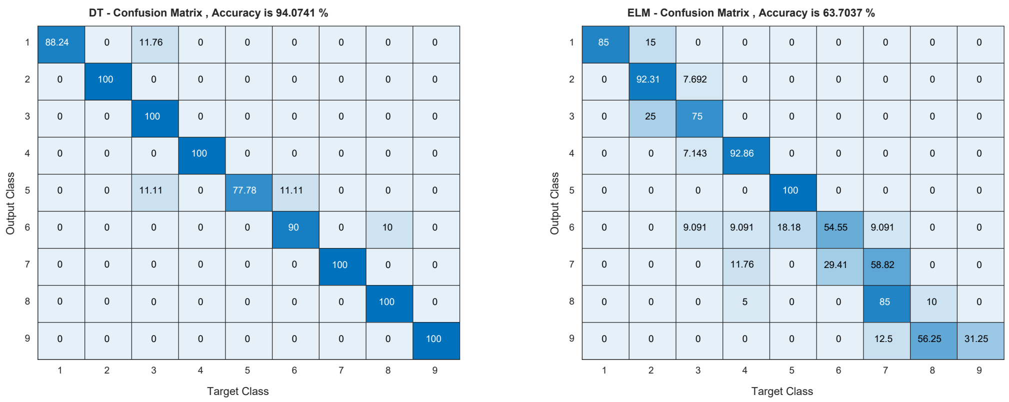

Figure 5.8: Confusion matrix of each classification method in the 6th experiment. (That of KNN, That of SVM, That of SOF, That of DRB, That of ERT, That of RF, That of DT and That of ELM).

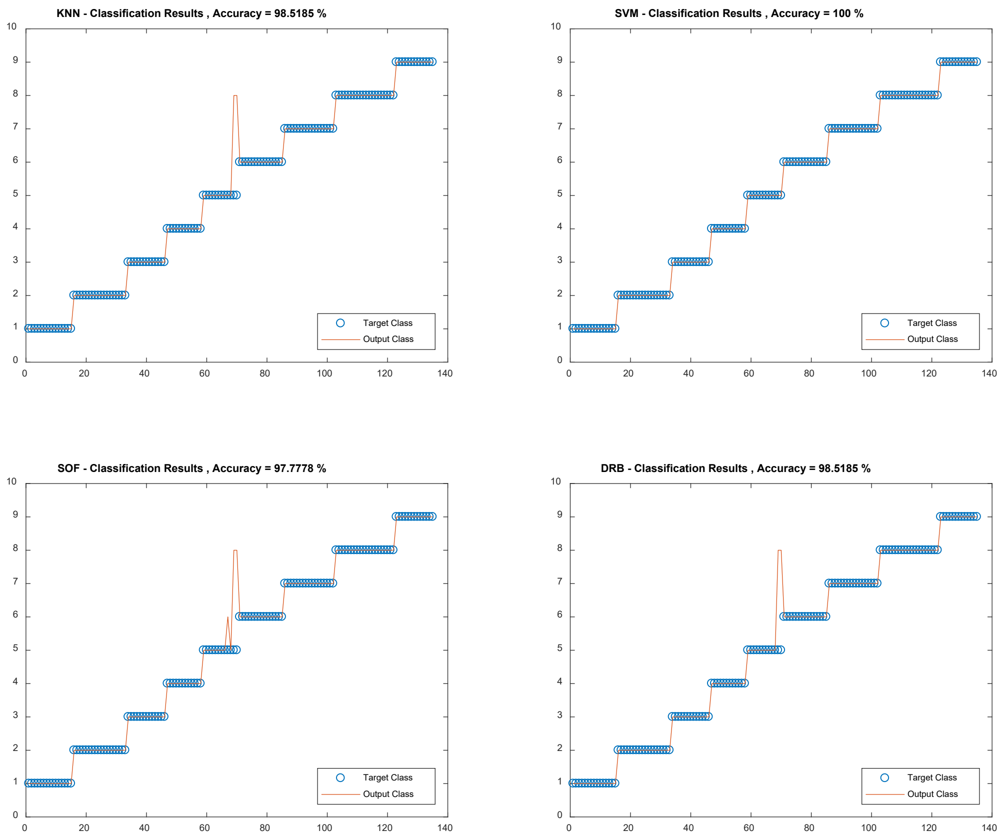

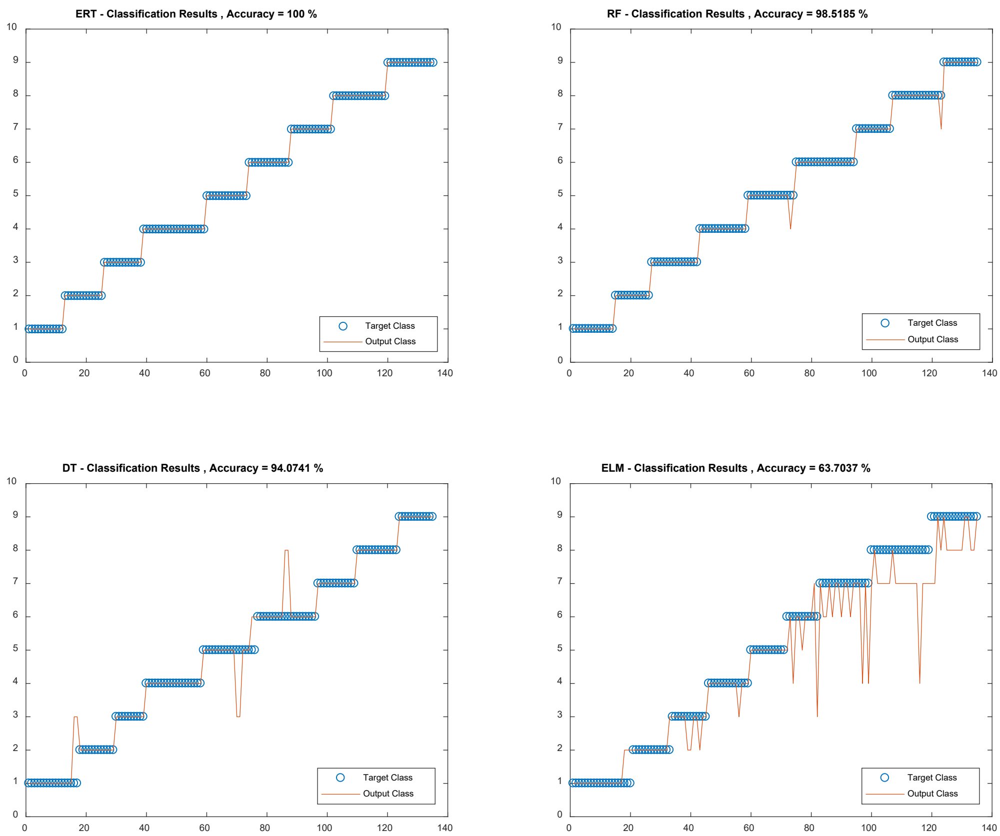

Figure 5.9: The classification results of the tested methods (KNN, SVM, SOF, DRB, ERT, RF, DT, and ELM) in the sixth experiment.

The ELM confusion matrix results clearly show that, at 63.703%, ELM has the lowest classification accuracy. Furthermore, it is evident that only in category 5 does ELM attain appropriate classification.

Of the testing samples, 5.9259% are misclassified according to the DT classification results. In particular, 11.76% of samples in category 1 are incorrectly assigned to category 3, 22.222% of samples in category 5 are incorrectly assigned to category 6, and 10% of samples in category 6 are incorrectly assigned to category 8.

A total of 2.222% of samples in the SOF classification results are incorrectly categorized, with 25% of category 5 samples being classified as categories 6 and 8. However, the misclassification rate of the KNN classifier is lower at 1.481%, with 16.67% of category 5 samples being classified as category 8 samples.

On the other hand, 1.481% of samples in the KNN, RF, and DRB classification findings are incorrectly classified. 16.67% of category 5 samples in the KNN and DRB cases are categorized as category 8. Nonetheless, 5.882% of category 8 samples are classified as category 7, and 6.25% of category 5 samples are classified as category 4. For RF.

There are no misclassified samples and 100% accuracy for both SVM and ERT classifiers. Although ERT and SVM have the same classification accuracy, it's crucial to remember that SVM performs better than ERT by 0.05 when it comes to the classification accuracy standard deviation (SVM: 0.07, ERT: 0.12). This suggests that SVM has better classification stability than ERT.

The advantage of SVM_PAM over ERT_PAM and other classifiers is highlighted by the findings from Table 6.6 and the examination of the Polygon Area Metric (PAM) box. The equal minimum value (0.993), mean value (0.998), and highest value (1) all demonstrate this. But the most significant distinction is found in the standard deviation (STD) value, as SVM has an STD of 0.1 whereas ERT has an STD of 0.02. This suggests that the SVM classifier is superior to the ERT classifier and also more stable.

The experimental results confirm that the suggested approach is a dependable and strong substitute for keeping an eye on the condition of electrical transformers, especially when it comes to fault identification and categorization.

5.4 Conclusion

This chapter presents a new method for electrical systems fault diagnostics that makes use of feature extraction methods and machine learning classifiers to identify various types of problems. The technique, which is based on infrared thermography (IRT), works well and provides a steady, non-intrusive, very sensitive method of detecting a variety of problems.

The first contribution uses an Extremely Randomized Trees (ERT) classifier with SURF-BoVW features extraction for problem identification in induction motors. The discovery of eight different stator fault types in induction motors, including the frequency of short circuits in each phase and the number of phases impacted by faults in the induction motor, serves as validation of the effectiveness of this approach.

The experimental results using the Extremely Randomized Trees (ERT) classifier show that the suggested method is a reliable substitute for tracking the condition of an induction motor when compared to other existing classifier methods. With the same inputs, the ERT classifier consistently outperforms Random Forest (RF) and shows better and more consistent classification effects. The suggested method provides superior classification accuracy and stability when compared to Support Vector Machine (SVM), Decision Tree (DT), K-Nearest Neighbor (KNN), Least Squares Support Vector Machine (LSSVM), and Deep Rule-Based (DRB). Because of this, it can diagnose induction motor problems with 100% classification precision.

The Polygon Area Metric (PAM) is used to assess the suggested approach, and the outcomes clearly show how much of each classification method's PAM is covered. Out of all the classifiers, ERT's Polygon Area Metric is the most advantageous.

In the second contribution, the GIST algorithm and SVM classifier serve as the foundation for the fault diagnosis technique for electrical transformers. Nine different electrical transformer states, including one healthy state and eight states with short-circuit defects in the common core winding, are successfully identified, demonstrating the efficacy of this approach. The experimental findings produced by the SVM classifier indicate that the suggested approach functions as a dependable substitute for other current classifiers when it comes to monitoring the state of electrical transformers.

The SVM classifier consistently performs better and has more stable classification effects when given consistent inputs. The suggested technique shows better classification accuracy and stability when compared to ERT, RF, DT, KNN, SOF, and DRB, making it a better option for fault identification in electrical transformers.

Chapter 6: Conclusion and Further Scope

This thesis explored the integration of infrared thermography and artificial intelligence for the diagnosis of faults in electromechanical systems ((induction motors, electrical transformers). The primary objective was to develop a robust framework combining the thermal imaging capabilities of infrared thermography with the analytical power of artificial intelligence to improve the accuracy and efficiency of fault detection and diagnosis. The research conducted demonstrated the potential of this integrated approach to transform traditional fault diagnosis methods and significantly improve the reliability and operational efficiency of electromechanical systems.

The main concluding remarks are summarized as follows:

- The use of infrared thermography has proven to be an effective non-destructive technique for fault detection and thermal behavior monitoring of electromechanical systems. It allows early detection of thermal anomalies that may indicate potential faults such as overheating, poor electrical connections or mechanical wear.Thermal images captured by thermography provide valuable data that can be analyzed to identify problem areas before they develop into critical failures.
- Artificiel intelligence algorithms, particularly machine learning and ensemble learning models, have shown significant promise in analyzing thermographic data. These algorithms can identify patterns and anomalies that are indicative of faults, often with greater accuracy and speed than traditional manual inspection methods. The ability of artificiel intelligence to process large datasets and continuously learn from new data enhances its diagnostic capabilities over time, making it a powerful tool for the faults diagnosis of electomechanical systems.
- The first contribution uses an Extremely Randomized Trees classifier with SURF-BoVW features extraction for problem identification in induction motors. The discovery of eight different stator fault types in induction motors, including the frequency of short circuits in each phase and the number of phases impacted by faults in the induction

motor, serves as validation of the effectiveness of this approach. The experimental results using the Extremely Randomized Trees classifier show that the suggested method is a reliable substitute for tracking the condition of an induction motor when compared to other existing classifier methods.

- In the second contribution, the GIST algorithm and SVM classifier serve as the foundation for the fault diagnosis technique for electrical transformers. Nine different electrical transformer states, including one healthy state and eight states with short-circuit defects in the common core winding, are successfully identified, demonstrating the efficacy of this approach. The experimental findings produced by the SVM classifier indicate that the suggested approach functions as a dependable substitute for other current classifiers when it comes to monitoring the state of electrical transformers.
- The Polygon Area Metric (PAM) is used to assess the suggested approach, and the outcomes clearly show how much of each classification method's PAM is covered. where the propose method's Polygon Area Metric is the most advantageous.

- The experimental result confirm that, the proposed method can be considered as a reliable alternative and robustness to monitor the state of both induction motors and electrical transformers fault detection and classification.

The contributions of this thesis are manifold:

- Innovation in Fault Diagnosis: By combining thermography and artificial intelegence, this research introduces a novel method for fault diagnosis that is both efficient and accurate. This approach represents a significant advancement over traditional techniques.
- Enhanced Maintenance Strategies: The ability to detect and diagnose faults early allows for the implementation of predictive maintenance strategies. This can lead to reduced maintenance costs, extended equipment life, and improved system reliability.
- Wide applicability: The framework developed in this thesis demonstrates that the proposed method is successfully applicable to fault detection of motors and transformers and can be adapted to other types of electromechanical systems in different industries, making it a versatile tool for fault diagnosis and maintenance.

In conclusion, this thesis has demonstrated the significant potential of integrating infrared thermography and artificial intelligence for the fault diagnosis of electromechanical systems. The innovative approach developed and validated through this research offers a powerful tool for enhancing the reliability, efficiency, and safety of industrial operations. By addressing current limitations and exploring new opportunities, this integrated methodology holds promise for the future of fault diagnosis and predictive maintenance in a wide range of applications.

Further Scope

While this thesis has laid the groundwork for integrating thermography and artificial intelligence in fault diagnosis, several areas for future research and development have been identified:

- User-Friendly Interfaces: Developing user-friendly interfaces and visualization tools to make the system more accessible to maintenance personnel and engineers without specialized knowledge in thermography or artificial intelligence.
- Extend the application of the proposed method based on thermography and artificial intelligence on other electromechanical equipment or sensitive components such as bearings, gears, etc.

References

[1] LEFFLER, Jan et TRNKA, Pavel. Failures of Electrical Machines-Review. In: 2022 8th International Youth Conference on Energy (IYCE). IEEE, 2022. p. 1-4.

[2] Mohamed Zair, Chemseddine Rahmoune, Djamel Benazzouz (2019) Multi-fault diagnosis of rolling bearing using fuzzy entropy of empirical mode decomposition, principal component analysis, and SOM neural network. Mechanical Engineering Science 0(0) 1–12.

[3] Toufik Bettahar, Chemseddine Rahmoune, Djamel Benazzouz and Boualem Merainani (2020) New method for gear fault diagnosis using empirical wavelet transform, Hilbert transform, and cosine similarity metric, Advances in Mechanical Engineering,Vol.12(6)1–11.

[4] B. R. Nayana and P. Geethanjali (2017) Analysis of Statistical Time-Domain Features Effectiveness in Identification of Bearing Faults From Vibration Signal, IEEE Sensors Journal, vol. 17, no. 17.

[5] Adam glowacz , witold glowacz, jarosław kozik, krzysztof piech, miroslav gutten, wahyu caesarendra, hui liu, frantisek brumercik , muhammad irfan, and z. faizal khan (2019) detection of deterioration of three-phase induction motor using vibration signals, measurement science review, 19, no. 6, 241-249.

[6] Yuhang Shi, Shengchang Ji, Fan Zhang, Fuqiang Ren, Lingyu Zhu, and Liang Lv, Multi-Frequency Acoustic Signal Under Short-Circuit Transient and Its Application on the Condition Monitoring of Transformer Winding, IEEE TRANSACTIONS ON POWER DELIVERY, VOL. 34, NO. 4, AUGUST 2019.

[7] Alexander Yu. Khrennikov, Fault Detection of Electrical Equipment. Diagnostic Methods, International Journal of Automation and Control Engineering Volume 2 Issue 1, February 2013.

[8] Alexandr A. Drobyshevski, Assessment of Transformer Winding Mechanical Condition by Low-Voltage Impulse Method, Paper accepted for presentation at 2003 IEEE Bologna PowerTech Conference, June 23-26, Bologna, Italy.

[9] Ou, Xiao-Bo, Ji, Sheng-Chang, Wang, Chun-Jie, Simulation of transformer short circuit reactance with FEM by coupling magnetic field with electric circuit, Gaoya Dianqi/High Voltage Apparatus, 46 (3) , 59-63, 2010.

[10] Bagheri, M., Naderi, M. S., Blackburn, T., & Phung, T. (2013). Frequency response analysis and short-circuit impedance measurement in detection of winding deformation within power transformers. IEEE Electrical Insulation Magazine, 29(3), 33-40.

[11] Liu, Y., Ji, S., Yang, F., Cui, Y., Zhu, L., Rao, Z., Yang, X. (2015). A study of the sweep frequency impedance method and its application in the detection of internal winding short circuit faults in power transformers. IEEE Transactions on Dielectrics and Electrical Insulation, 22(4), 2046-2056.

[12] Khmais Bacha, Seifeddine Souahlia, Moncef Gossa, Power transformer fault diagnosis based on dissolved gas analysis by support vector machine. Electric Power Systems Research 83 (2012) 73, 79.

[13] Wojciech Sikorski, Development of Acoustic Emission Sensor Optimized for Partial Discharge Monitoring in Power Transformers, Sensors 2019, 19, 1865; doi:10.3390/s19081865.

[14] USAMENTIAGA, Rubén, VENEGAS, Pablo, GUEREDIAGA, Jon, et al. Infrared thermography for temperature measurement and non-destructive testing. Sensors, 2014, vol. 14, no 7, p. 12305-12348.

[15] Ibarra-Castanedo, C.; Tarpani, J.R.; Maldague, X.P. Nondestructive testing with thermography. Eur. J. Phys. 2013, 34, S91.

[16] Bagavathiappan, S.; Lahiri, B.; Saravanan, T.; Philip, J.; Jayakumar, T. Infrared thermography for condition monitoring, A review. Infrared Phys. Technol. 2013, 60,35–55.

[17] SARAWADE, Akshay A. et CHARNIYA, Nadir N. Infrared thermography and its applications: A review. In: 2018 3rd International conference on communication and electronics systems (ICCES). IEEE, 2018. p. 280-285.

[18] Badulescu, C.; Gr´ediac, M.; Haddadi, H.; Mathias, J.D.; Balandraud, X.; Tran, H.S. Applying the grid method and infrared thermography to investigate plastic deformation in aluminium multicrystal. Mech. Mater. 2011, 43, 36–53.

[19] C. Meola, Origin and theory of infrared thermography, in: C. Meola (Ed.), Infrared Thermography Recent Advances and Future Trends, Bentham Books, 2012, pp. 3–28.

[20] M. Rai, T. Maity, R. K. Yadav, “Thermal imaging system and its real time applications: a survey,” Journal of Engineering Technology, vol. 6, issue 2, pp. 290-303, 2017.

[21] B. Lahiri, S. Bagavathiappan, T. Jayakumar, and J. Philip, “Medical applications of infrared thermography: A review,” Infrared Physics & Technology, vol.55, no. 4, pp. 221-235, 2012.

[22] R. Gade and T. B. Moeslund, “Thermal cameras and applications: a survey,” Machine Vision and Applications, vol. 25, no. 1, pp. 245-262, Sep. 2013.

[23] R. Vadivambal, D. S. Jayas, “Applications of Thermal Imaging in Agriculture and Food Industry - A Review,” Food and Bioprocess Technology, vol. 4, pp. 186-199, 2011.

[24] M. Stumper and J. Kraus “Thermal imaging in aviation,” Magazine of Aviation Development, vol. 3, no. 16, pp. 13-16, 2015.

[25] R. Gade and T. B. Moeslund, “Thermal cameras and applications: a survey,” Machine Vision and Applications, vol. 25, no. 1, pp. 245-262, Sep. 2013.

[26] Zhang, Y., et al. (2021). *IEEE Transactions on Industrial Electronics*, 68(6), 4791-4802.

[27] Li, W., et al. (2020). *Mechanical Systems and Signal Processing*, 138, 106577.

[28] Sun, X., et al. (2020). *Infrared Physics & Technology*, 109, 103352.

[29] XIA, Changjie, REN, Ming, WANG, Bing, *et al.* Infrared thermography-based diagnostics on power equipment: State-of-the-art. *High Voltage*, 2021, vol. 6, no 3, p. 387-407.

[30] HAN, Sheng, YANG, Fan, JIANG, Hui, *et al.* A smart thermography camera and application in the diagnosis of electrical equipment. *IEEE Transactions on Instrumentation and Measurement*, 2021, vol. 70, p. 1-8.

[31] Zhou, S., et al. (2021). *IEEE Transactions on Industrial Informatics*, 17(6), 4188-4200.

[32] KESZTYÜS, Dorothea, BRUCHER, Sabrina, et KESZTYÜS, Tibor. Use of infrared thermography in medical diagnostics: A scoping review protocol. *BMJ open*, 2022, vol. 12, no 4, p. e059833.

[33] CHOUDHARY, Anurag, GOYAL, Deepam, et LETHA, Shimi Sudha. Infrared thermography-based fault diagnosis of induction motor bearings using machine learning. *IEEE Sensors Journal*, 2020, vol. 21, no 2, p. 1727-1734. [34] Chen, Y., et al. (2019). *Journal of Physics: Conference Series*, 1320(1), 012008.

[35] DU, Bolun, HE, Yigang, HE, Yunze, *et al.* Progress and trends in fault diagnosis for renewable and sustainable energy system based on infrared thermography: A review. *Infrared Physics & Technology*, 2020, vol. 109, p. 103383.

[36] LI, Xiaoyuan, YING, Xiaowei, ZHU, Wen, et al. Nondestructive detection and analysis based on data enhanced thermography. Measurement Science and Technology, 2022, vol. 33, no 6, p. 064006.

[37] Zhen Jia, Zhenbao Liu, Chi-Man Vong, and Michael Pecht (2019) A Rotating Machinery Fault Diagnosis Method Based on Feature Learning of Thermal Images. DOI 10.1109/ACCESS.2019.2893331, IEEE Access.

[38] Bei Xie, Jiaohua Qin, Xuyu Xiang, Hao Li and Lili Pan, An Image Retrieval Algorithm Based on GIST and SIFT Features, International Journal of Network Security, Vol.20, No.4, PP.609-616, July 2018 (DOI: 10.6633/IJNS.201807 20(4).02)

[39] XIA, Changjie, REN, Ming, WANG, Bing, et al. Infrared thermography-based diagnostics on power equipment: State-of-the-art. High Voltage, 2021, vol. 6, no 3, p. 387-407.

[40] DU, Bolun, HE, Yigang, HE, Yunze, et al. Progress and trends in fault diagnosis for renewable and sustainable energy system based on infrared thermography: A review. Infrared Physics & Technology, 2020, vol. 109, p. 103383.

[41] STAFFORD, Imogen S., KELLERMANN, Melina, MOSSOTTO, Enrico, et al. A systematic review of the applications of artificial intelligence and machine learning in autoimmune diseases. NPJ digital medicine, 2020, vol. 3, no 1, p. 30.

[42] FERNANDES, Marta, CORCHADO, Juan Manuel, et MARREIROS, Goreti. Machine learning techniques applied to mechanical fault diagnosis and fault prognosis in the context of real industrial manufacturing use-cases: a systematic literature review. Applied Intelligence, 2022, vol. 52, no 12, p. 14246-14280.

[43] BERTOLINI, Massimo, MEZZOGORI, Davide, NERONI, Mattia, et al. Machine Learning for industrial applications: A comprehensive literature review. Expert Systems with Applications, 2021, vol. 175, p. 114820.

[44] KHAN, Muzammil, MEHRAN, Muhammad Taqi, HAQ, Zeeshan Ul, et al. Applications of artificial intelligence in COVID-19 pandemic: A comprehensive review. Expert systems with applications, 2021, vol. 185, p. 115695.

[45] KUMBURE, Mahinda Mailagaha, LOHRMANN, Christoph, LUUKKA, Pasi, et al. Machine learning techniques and data for stock market forecasting: A literature review. Expert Systems with Applications, 2022, vol. 197, p. 116659.

[46] MAULUD, Dastan et ABDULAZEEZ, Adnan M. A review on linear regression comprehensive in machine learning. Journal of Applied Science and Technology Trends, 2020, vol. 1, no 2, p. 140-147.

[47] ELTOUNY, Kareem, GOMAA, Mohamed, et LIANG, Xiao. Unsupervised learning methods for data-driven vibration-based structural health monitoring: a review. Sensors, 2023, vol. 23, no 6, p. 3290.

[48] ZHANG, Yuzhen, LIU, Jingjing, et SHEN, Wenjuan. A review of ensemble learning algorithms used in remote sensing applications. Applied Sciences, 2022, vol. 12, no 17, p. 8654.

[49] SALEM, Hanaa, SHAMS, Mahmoud Y., ELZEKI, Omar M., et al. Fine-tuning fuzzy KNN classifier based on uncertainty membership for the medical diagnosis of diabetes. Applied Sciences, 2022, vol. 12, no 3, p. 950.

[50] KHERIF, Omar, BENMAHAMED, Youcef, TEGUAR, Madjid, et al. Accuracy improvement of power transformer faults diagnostic using KNN classifier with decision tree principle. IEEE Access, 2021, vol. 9, p. 81693-81701.

[51] Pierre Geurts, Damien Ernst, Louis Wehenkel (2006) Extremely randomized trees, Mach Learn 63: 3–42.

[52] Marée, R., Geurts, P. & Wehenkel, L. (2007) Random subwindows and extremely randomized trees for image classification in cell biology. BMC Cell Biol 8, S2. https://doi.org/10.1186/1471-2121-8-S1-S2.

[53] Vladimir Vapnik, Corinna Cortes, Support-Vector Networks, Machine Learning, 20, 273-297 (1995)

[54] AYDEMIR, Onder. A new performance evaluation metric for classifiers: polygon area metric. Journal of Classification, 2021, vol. 38, no 1, p. 16-26.

[55] Najafi, Mohamad; Baleghi, Yasser; Mirimani, Seyyed Mehdi (2020) Thermal image of equipment (Induction Motor), Mendeley Data, V1, doi: 10.17632/m4sbt8hbvk.1.

[56] Najafi, Mohamad; Baleghi, Yasser; Mirimani, Seyyed Mehdi (2020), “Thermal images_1-phase_ dry type_Transformer”, Mendeley Data, V1.